

# 1 Transcriptome and histone epigenome of *Plasmodium vivax* 2 salivary-gland sporozoites point to tight regulatory control 3 and potential mechanisms for liver-stage differentiation.

4  
5 Vivax Sporozoite Consortium\* (Ivo Muller<sup>1,2,3</sup>, Aaron R. Jex<sup>1,3,4</sup>, Stefan H. I. Kappe<sup>5</sup>,  
6 Sebastian A. Mikolajczak<sup>5</sup>, Jetsumon Sattabongkot<sup>7</sup>, Rapatbhorn Patrapuvich<sup>6</sup>, Scott  
7 Lindner<sup>8</sup>, Erika L. Flannery<sup>5</sup>, Cristian Koepfli<sup>1</sup>, Brendan Ansell<sup>4</sup>, Anita Lerch<sup>1</sup>, Samantha J  
8 Emery-Corbin<sup>1</sup>, Sarah Charnaud<sup>1</sup>, Jeffrey Smith<sup>1</sup>, Nicolas Merrienne<sup>2</sup>, Kristian E.  
9 Swearingen<sup>5</sup>, Robert L. Moritz<sup>9</sup>, Michaela Petter<sup>10,11</sup>, Michael Duffy<sup>10</sup>, Vorada Chuenchob<sup>5</sup>).

10 \*Group authorship – all authors are equal contributors (order per author contributions section below).

- 11 1. Population Health and Immunity Division, The Walter and Eliza Hall Institute for Medical Research, 1G Royal Parade,  
12 Parkville, Victoria, 3052, Australia.
- 13 2. Malaria: Parasites & Hosts Unit, Institut Pasteur, 28 Rue de Dr. Roux, 75015, Paris, France.
- 14 3. Department of Medical Biology, The University of Melbourne, Victoria, 3010, Australia.
- 15 4. Faculty of Veterinary and Agricultural Sciences, The University of Melbourne, Corner of Park and Flemington Road,  
16 Parkville, Victoria, 3010, Australia.
- 17 5. Center for Infectious Disease Research, 307 Westlake Avenue North, Suite 500, Seattle, WA 98109, USA;
- 18 6. Department of Global Health, University of Washington, Seattle, WA 98195, USA.
- 19 7. Mahidol *Vivax* Research Center, Faculty of Tropical Medicine, Mahidol University, Bangkok 10400, Thailand.
- 20 8. Department of Biochemistry and Molecular Biology, Center for Malaria Research, Pennsylvania State University, University  
21 Park, PA 16802, USA.
- 22 9. Institute for Systems Biology, Seattle, WA, 98109, USA.
- 23 10. Department of Medicine Royal Melbourne Hospital, The Peter Doherty Institute, The University of Melbourne, 792  
24 Elizabeth Street, Melbourne, Victoria 3000, Australia.
- 25 11. Institute of Microbiology, University Hospital Erlangen, Erlangen 91054, Germany

## 26 27 28 **ABSTRACT**

29 *Plasmodium vivax* is the key obstacle to malaria elimination in Asia and Latin America,  
30 largely attributed to its ability to form resilient hypnozoites (sleeper-cells) in the host liver  
31 that escape treatment and cause relapsing infections. The decision to form hypnozoites is  
32 made early in the liver infection and may already be set in sporozoites prior to invasion. To  
33 better understand these early stages of infection, we undertook a comprehensive  
34 transcriptomic and histone epigenetic characterization of *P. vivax* sporozoites. The salivary-  
35 gland sporozoite transcriptome is heavily composed of transcripts associated with functions  
36 needed for early infection of the vertebrate host and development within hepatocytes.  
37 Through comparisons to recently published proteome data for the *P. vivax* sporozoite, our  
38 study finds that although highly transcribed, these transcripts are not detectable as proteins  
39 and may be regulated through translational repression; a finding we test for a small subset of  
40 transcripts and proteins through immunofluorescent microscopy of sporozoites and liver  
41 stages in humanized mice. We identify differential transcription between the sporozoite and  
42 published transcriptomes of asexual blood-stages and mixed versus hypnozoite-enriched liver  
43 stages. These comparisons point to multiple layers of transcriptional, post-transcriptional and  
44 post-translational control that appear active in sporozoites and to a lesser extent hypnozoites,  
45 but largely absent in replicating liver schizonts or mixed blood-stages. Common transcripts  
46 up-regulated in sporozoites and hypnozoites compared to mixed (i.e., schizont) liver-stages  
47 identify genes linked to dormancy/persistence in bacteria, amoebae and plants. We also  
48 characterise histone epigenetic modifications in the *P. vivax* sporozoite and explore their role  
49 in regulating transcription. Collectively, these data support the hypothesis that the sporozoite  
50 as a tightly programmed stage primed to infect the human host and identifies potential  
51 mechanisms for hypnozoite-formation that may be further explored in liver stage models.

## 52 53 **INTRODUCTION**

54 Malaria is among the most significant infectious diseases impacting humans globally, with  
55 3.3 billion people at risk of infection, 381 million suspected clinical cases and up to ~660,000  
56 deaths attributed to malaria in 2014 [1]. Two major parasitic species contribute to the vast  
57 majority of human malaria, *Plasmodium falciparum* and *P. vivax*. Historically, *P. falciparum*  
58 has attracted the majority of global attention, due to its higher contribution to morbidity and

59 mortality. However, *P. vivax* is broadly distributed, more pathogenic than previously thought,  
60 and is recognised as the key obstacle to malaria elimination in the Asia-Pacific and Americas  
61 [2]. Unlike *P. falciparum*, *P. vivax* can establish long-lasting ‘sleeper-cells’ (= hypnozoites)  
62 in the host liver that emerge weeks, months or years after the primary infection (= relapsing  
63 malaria) [3]. Primaquine is the only approved drug that prevents relapse. However, the short  
64 half-life, long dosage regimens and incompatibility of primaquine with glucose-6-phosphate-  
65 dehydrogenase deficiency (which requires pre-screening of recipients [4]) makes it unsuitable  
66 for widespread use. As a consequence, *P. vivax* is overtaking *P. falciparum* as the primary  
67 cause of malaria in a number of co-endemic regions [5]. Developing new tools to diagnose,  
68 treat and/or prevent hypnozoite infections is considered one of the highest priorities in the  
69 malaria elimination research agenda [6].

70 When *Plasmodium* sporozoites are deposited by an infected mosquito, they likely  
71 traverse the skin cells, enter the blood-stream and are trafficked to the host liver, as has been  
72 shown in rodents [7]. The sporozoites’ journey from skin deposition to hepatocytes takes less  
73 than a few minutes [8]. Upon reaching the liver, sporozoites traverse Kupffer and endothelial  
74 cells to reach the parenchyma, moving through several hepatocytes before invading a final  
75 hepatocyte suitable for development [7, 9]. Within hepatocytes, these parasites replicate, and  
76 undergo further development and differentiation to produce merozoites that emerge from the  
77 liver and infect red blood cells. However, *P. vivax* sporozoites are able to commit to two  
78 distinct developmental fates within the hepatocyte: they either immediately continue  
79 development as replicating schizonts and establish a blood infection, or delay replication and  
80 persist as hypnozoites. Regulation of this major developmental fate decision is not understood  
81 and this represents a key gap in current knowledge of *P. vivax* biology and control.

82 Sporozoites prepare for mammalian host infection while still residing in the mosquito  
83 salivary glands. It has been hypothesized that *P. vivax* sporozoites exist within an inoculum as  
84 replicating ‘tachysporozoites’ and relapsing ‘bradysporozoites’ [10] and that these  
85 subpopulations may have distinct developmental fates as schizonts or hypnozoites, thus  
86 contributing to their relapse phenotype [10-12]. This observation is supported by the stability  
87 of different hypnozoite phenotypes (ratios of hypnozoite to schizont formation) in *P. vivax*  
88 infections of liver-chimeric mouse models [13]. To determine fates in the sporozoite stage  
89 control of protein expression must take place. Studies using rodent malaria parasites have  
90 identified genes [14] that are transcribed in sporozoites but translationally repressed (i.e.,  
91 present as transcript but un- or under-represented as protein), via RNA-binding proteins [15],  
92 and ready for immediate translation after the parasites’ infection of the mammalian host cell  
93 [13, 16]. It is therefore also possible that translational repression (i.e., the blocking of  
94 translation of present and retained transcripts) and other mechanisms of epigenetic control  
95 may contribute to the *P. vivax* sporozoite fate decision and hypnozoite formation, persistence  
96 and activation. Supporting this hypothesis, histone methyltransferase inhibitors stimulate  
97 increased activation of *P. cynomolgi* hypnozoites to become schizonts in macaque  
98 hepatocytes [17, 18]. Epigenetic control of stage development is further evidenced in  
99 *Plasmodium* through chromatin structure controlling expression of PfAP2-G, a specific  
100 transcription factor that, in turn, regulates gametocyte (dimorphic sexual stages) development  
101 in blood-stages [19]. It is well documented that *P. vivax* hypnozoite activation patterns  
102 stratify with climate and geography [11] and recent modelling suggests transmission potential  
103 selects for hypnozoite phenotype [20]. Clearly the ability for *P. vivax* to dynamically regulate  
104 hypnozoite formation and relapse phenotypes in response to high or low transmission periods  
105 in different climate conditions would confer a significant evolutionary advantage.

106 Unfortunately, despite recent advances [21] current approaches for *in vitro* *P. vivax*  
107 culture do not support routine maintenance in the laboratory and tools to directly perturb gene  
108 function are not established. This renders studies on *P. vivax*, particularly its sporozoites and  
109 liver stages, exceedingly difficult. Although *in-vitro* liver stage assays and humanised mouse  
110 models are being developed [13], ‘omics analysis of *P. vivax* liver stage dormancy has until  
111 recently [22] been impossible and even now is in its early stages. Recent characterization [23]  
112 of liver-stage (hypnozoites and schizonts) of *P. cynomolgi* (a related and relapsing parasite in  
113 macaques) provides valuable insight, but investigations in *P. vivax* directly are clearly

114 needed. The systems analysis of *P. vivax* sporozoites that reside in the mosquito salivary  
115 glands and are poised for transmission and liver infection offer a key opportunity to gain  
116 insight into *P. vivax* infection. *Plasmodium vivax* sporozoites have been explored previously  
117 by microarray [24] and most recently, in a single RNA-seq replicate [25] and a study on  
118 sporozoite activation [Roth, 2018 #66]. Epigenetic regulation in sporozoites has only been  
119 explored in *P. falciparum* [26, 27]. Here, we present a detailed characterization of the *P. vivax*  
120 sporozoite transcriptome and histone epigenome and use these data to better understand this  
121 key infective stage and the role of sporozoite programming in invasion and infection of the  
122 human host, and development within the host liver.

123

## 124 RESULTS AND DISCUSSION

125 Mosquito infections were generated by membrane feeding of blood samples taken from *P.*  
126 *vivax* infected patients in western Thailand (n = 9). Approximately 3-15 million *P. vivax*  
127 sporozoites were harvested per isolate from *Anopheles dirus* salivary glands. Using RNA-seq,  
128 we detected transcription for 5,714 *P. vivax* genes (based on the *P. vivax* P01 gene models:  
129 [28]) and obtained a high degree of coverage (4,930 with a mean counts per million (CPM)  $\geq$   
130 1.0; Figure S1 and Table S1 and S2). Among the most highly transcribed genes in the  
131 infectious sporozoite stage are *csp* (circumsporozoite protein), five *etramps* (early transcribed  
132 membrane proteins), including *uis3* (up-regulated in infective sporozoites), *uis4* and *lsap-1*  
133 (liver stage associated protein 1), a variety of genes involved in cell transversal and initiation  
134 of invasion, including *celtos* (cell traversal protein for ookinetes and sporozoites), *gest*  
135 (gamete egress and sporozoite traversal protein), *spect1* (sporozoite protein essential for cell  
136 traversal) and *siap-1* (sporozoite invasion associated protein), and genes associated with  
137 translational repression (*alba1*, *alba4* and *Puf2*). Collectively, these genes account for  $>1/3^{\text{rd}}$   
138 of all transcripts in the sporozoite. Although we found only moderate agreement ( $R^2 = 0.35$ ;  
139 Figure S2) between our RNA-seq data and previous microarray data for *P. vivax* sporozoites  
140 and blood-stages [24], improved transcript detection and quantitation is expected with the  
141 increased technical resolution of RNA-seq over microarray. Supporting this, we find higher  
142 correlation between RNA-seq data from *P. vivax* and *P. falciparum* (single replicate  
143 sequenced herein for comparative purposes) sporozoite datasets ( $R^2 = 0.42$ ), compared to  
144 either species relative to published microarray data (Figure S2 and Table S3).

145 Although microarray supports the high transcription in sporozoites of genes such as  
146 *uis4*, *csp*, *celtos* and several other *etramps*, 27% and 16% of the most abundant 1% of  
147 transcribed genes in our sporozoite RNA-seq data are absent from the top decile or quartile  
148 respectively in the existing *P. vivax* sporozoite microarray data [24]. Among these are genes  
149 involved in early invasion/hepatocyte development, such as *lsap-1*, *celtos*, *gest* and *siap-1*, or  
150 translational repression (e.g., *alba-1* and *alba-4*); orthologs of these genes are also in the top  
151 percentile of transcripts in RNA-seq (see [26, 29]) and previous microarray data [30, 31] for  
152 human-infecting *P. falciparum* and murine-infecting *P. yoelii* sporozoites, suggesting many  
153 are indeed more abundant than previously characterized. A subset of representative  
154 transcripts, including *Pv\_AP2-X* (PVP01\_0733100), *d13*, *gest*, *g10* (PVP01\_1011100), 40S  
155 ribosomal protein S27 (PVP01\_1409300), *puf-2*, *zipco* and 14-3-3, were tested by qPCR for  
156 their transcript abundance relative to *celtos* and *sera* (Figure 1A and Table S4). This  
157 representative set differed markedly in their relative abundance between our RNAseq and  
158 previous microarray data [24]. To control for batch effects introduced by collection of the  
159 sporozoites used here for RNAseq, this testing was conducted in an additional six sample  
160 replicates representing four additional clinical *P. vivax* isolates (PvSPZ-Thai13-16; with  
161 PvSPZ-Thai16 tested in technical triplicate). The qPCR results agreed with the RNAseq data  
162 for these transcripts (Table S4).

163

164 **Transcription in *P. vivax* relative to other plasmodia sporozoites.** To gain insight into  
165 species-specific aspects of the *P. vivax* transcriptome, we qualitatively compared these data  
166 with available data for *P. falciparum* [27] and *P. yoelii* sporozoites (single replicate only) for  
167 4,067 single-copy orthologs (SCO) (transcribed at  $\geq 1$  TPM in *P. vivax* infectious  
168 sporozoites) shared with *P. falciparum* and *P. yoelii* (Table S5). Genes highly transcribed in

169 salivary-gland sporozoites of all three species include *celtos*, *gest*, *trap*, *siap1*, *spect1* and  
170 *puf2*. There are 696 *P. vivax* genes shared as orthologs between *P. vivax* P01 and *P. vivax*  
171 Sall1 lacking a defined SCO in *P. falciparum* or *P. yoelli* transcribed at a mean of  $\geq 1$  TPM in  
172 *P. vivax* salivary-gland sporozoites (Table S6). Prominent among these are *vir* (n=25) and *Pv-*  
173 *fam* (41 fam-e, 16 fam-b, 14 fam-a, 8 fam-d and 3 fam-h) genes, as well as hypothetical  
174 proteins or proteins of unknown function (n=212) and, interestingly, a number of ‘merozoite  
175 surface protein’ 3 and 7 homologs (n=5 of each). Both *msp3* and *msp7* have undergone  
176 significant expansion in *P. vivax* relative to *P. falciparum* and *P. yoelli* [32] and may have  
177 repurposed functions in sporozoites. In addition, there are 69 *P. vivax* P01 genes lacking a  
178 defined ortholog in *P. vivax* Sall1, *P. falciparum* or *P. yoelli* transcribed at  $\geq 1$  TPM in  
179 infectious *P. vivax* sporozoites; most of which are *Plasmodium* interspersed repeat (PIR)  
180 genes [32] found in telomeric regions of the P01 assembly and likely absent from the Sall1  
181 assembly but present in the Sall1 genome, indicating the improved coverage of telomeric  
182 regions in P01 relative to Sall1.

183

184 ***P. vivax* sporozoites transcriptome compared with proteome.** We compared relative  
185 protein abundance presented in a recently published *P. vivax* sporozoite proteome [33] to  
186 relative transcript abundance from the current study (Figure 1B and Table S7). The proteome  
187 study incorporated data from the same PvSPZ-Thai1 and PvSPZ-Thai5 isolates tested by  
188 RNAseq here. We identified 2,402 *P. vivax* genes transcribed in the sporozoite (CPM > 1) for  
189 which no protein expression was detected. Although many of these are lowly transcribed and  
190 likely below the detection sensitivity of LC-MS proteomics, others are among the most highly  
191 transcribed genes in the sporozoite, indicating these may be under translational repression.

192 Translational repression, the mechanism through which transcripts are held in stasis  
193 by RNA binding proteins, has been demonstrated to have important functional roles in the  
194 transition of *Plasmodium* spp. between the vertebrate to invertebrate host. More than 700  
195 genes have been identified as translationally repressed in *Plasmodium berghei* (‘rodent  
196 malaria’) gametocytes based on DOZI (DEAD box RNA helicase “development of zygote  
197 inhibited”) pulldowns [34]. Translational repression mechanisms mediated through Puf-2  
198 have been explored in sporozoites of several *Plasmodium* species and regulate some of the  
199 most abundant transcripts in the sporozoite, such as *uis-3* and *uis-4*. UIS3 and UIS4 are the  
200 best characterized proteins under translational repression by Puf-2 in sporozoites [35] and are  
201 essential for liver-stage development [14].

202 In considering genes that may be translationally repressed (i.e., transcribed but not  
203 translated) in the *P. vivax* sporozoite, we confine our observations to those transcripts  
204 representing the top decile of transcript abundance to ensure their lack of detection as proteins  
205 was not due to limitations in the detection sensitivity of the proteomic dataset. Approximately  
206 1/3<sup>rd</sup> of transcripts in the top decile of transcriptional abundance (n = 170 of 558) in *P. vivax*  
207 sporozoites were not detectable as peptides in multiple replicates (Figure 1B and Table S7).  
208 Of these 170 putatively repressed transcripts, 156 and 154 have orthologs in *P. falciparum*  
209 and *P. yoelli* respectively, with 89 and 118 of these also not detected as proteins in *P.*  
210 *falciparum* and *P. yoelli* salivary-gland sporozoites [36] despite being highly transcribed in  
211 these stages (see [26, 29]; Tables S3-S5), and 133 (78.2%) having no detectable sporozoite  
212 expression (>1 unique peptide count) in LC-MS data deposited for any species in PlasmoDB  
213 (Table S8). In contrast, 106 of these putatively repressed transcripts with orthologs in other  
214 *Plasmodium* species (Table S8) for which proteomic data is available in PlasmoDB, are  
215 detectable (>1 unique peptide count) by LC-MS methods in at least one other life-cycle stage,  
216 indicating against a technical issue (e.g., inability to be trypsin-digested) preventing their  
217 detection in the *P. vivax* sporozoite proteome [33]. In addition to *uis3* and *uis4*, genes  
218 involved in liver stage development and detectable as transcripts but not proteins in the *P.*  
219 *vivax* sporozoites include *lsap1* (liver stage associated protein 1), *zipco* (ZIP domain-  
220 containing protein), several other *etramps* (PVP01\_1271000, PVP01\_0422600,  
221 PVP01\_0504800 and PVP01\_0734800), *pv1* (parasitophorous vacuole protein 1) and *lisp1*  
222 and *lisp2* (PVP01\_1330800 and PVP01\_0304700). Also notable among genes detectable as  
223 transcripts but not proteins in sporozoites is a putative ‘Yippee’ homolog (PVP01\_0724100).

224 Yippee is a DNA-binding protein that, in humans (YPEL3), suppresses cell growth [37] and  
225 is regulated through histone acetylation [38], making it noteworthy in the context of *P. vivax*  
226 hypnozoite developmental arrest.

227 Although verifying each putatively repressed transcript will require further empirical  
228 data, our system level approach is supported by immunofluorescent microscopy (Figure 1C)  
229 of UIS4, LISP1, EXP1 and ACP (PVP01\_0416300). These represent one known and three  
230 putative (i.e., newly proposed here) translationally repressed genes in *P. vivax* sporozoites,  
231 and are compared to TRAP and BiP (which are both transcribed and expressed as protein in  
232 the *P. vivax* sporozoite; Table S8). The *lisp1* gene is an interesting find. In *P. berghei*, *lisp1* is  
233 essential for rupture of the PVM during liver stage development allowing release of the  
234 merozoite into the host blood stream. *Pv-lisp1* is ~350-fold and ~1,350-fold more highly  
235 transcribed in *P. vivax* sporozoites compared to sporozoites of either *P. falciparum* or *P.*  
236 *yoelii* (see Table S5). IFAs using LISP1 specific mAbs (Figure 1C) show that this protein is  
237 undetectable in sporozoites but clearly expressed at 7 days post-infection in liver schizonts.  
238

### 239 **Up-regulated transcripts in *P. vivax* sporozoites relative to other life-cycle stages.**

240 Recently completed studies of the transcriptome of *P. vivax* for sporozoite activation [39], as  
241 well as, liver [22] and asexual blood-stages [40] support comparative transcriptomic study of  
242 sporozoites, their biology and transcriptional regulation over the *P. vivax* life-cycle. Recently  
243 published data for activate sporozoites from Roth et al [39] was significantly lower depth  
244 coverage, with ~0.03 to 0.6M reads mapped the *P. vivax* P01 coding domains; compared with  
245 0.7 to 15.3 M, 2.4 to 10.6 M and 18.7 to 57.6M mapped reads for salivary sporozoite, liver-  
246 stages [22] and asexual blood stages [40] respectively. This lower coverage could not be  
247 compensated for through data normalization and therefore data from Roth et al [39] was not  
248 included in our quantitative analyses, although qualitatively, many of the highly transcribed  
249 genes in Roth et al [39] sporozoites were among the highly transcribed genes in salivary  
250 sporozoites from the present study. The remaining RNAseq data presents an analytical  
251 challenge in that each (sporozoites, liver-stages and blood stages) is produced in a separate  
252 study and may be influenced by technical batch effects that cannot be differentiated from  
253 biologically meaningful changes. To address this, we first examined *P. vivax* transcripts in a  
254 previous microarray study of multiple *P. vivax* life-cycle stages [24], including sporozoites  
255 and several blood-stages, to identify genes that may be transcriptionally stable across the life-  
256 cycle. We identified ~160 genes with low transcriptional variability between sporozoites and  
257 blood-stages that covered the breadth of transcript abundance levels in Westenberger et al  
258 [24]. These include genes typically associated with “house-keeping” functions, such as  
259 ribosomal proteins, histones, translation initiation complex proteins and various chaperones  
260 (see Figure S3 and Table S8). We assessed transcription of these 160 genes among the current  
261 and recently published RNA-seq data for *P. vivax* and all were of similarly low variability  
262 (Figure S4). This suggests that any batch effect between the studies is sufficiently lower than  
263 the biological differences between each life-cycle stage, allowing informative comparisons.  
264 We then combined all published RNAseq-based, transcriptomic data available for *P. vivax*  
265 [22, 39, 40] with the salivary sporozoite data generated here.  
266

267 ***P. vivax* sporozoite relative to blood-stage transcriptome.** To identify transcripts up-  
268 regulated in sporozoites, we first compared the *P. vivax* sporozoite transcriptome to RNA-seq  
269 data for *P. vivax* blood-stages [40] (Figure 2 and Figures S7-S10). We identified 1,672 up  
270 (Table S9); Interactive Glimma Plot - Supplementary Data 1) and 1,958 down-regulated  
271 (Table S9); Interactive Glimma Plot - Supplementary Data 1) transcripts (FDR  $\leq$  0.05;  
272 minimum 2-fold change in Counts per Million (CPM)) and explored patterns among these  
273 differentially transcribed genes (DTGs) by protein family (Figure 2C and Table S10) and  
274 Gene Ontology (GO) classifications (Table S11). RNA recognition motifs (RRM-1 and  
275 RRM-6) and helicase domains (Helicase-C and DEAD box helicases) are over-represented  
276 (p-value  $<$ 0.05) among transcripts up-regulated in sporozoites, consistent with translational  
277 repression through ribonucleoprotein (RNP) granules [41]. Transcripts encoding nucleic acid  
278 binding domains, such as bromodomains (PF00439; which can also bind lysine-acetylated

279 proteins), zinc fingers (PF13923) and EF hand domains (PF13499) are also enriched in  
280 sporozoites. Included among these proteins are a putative ApiAP2 transcription factor  
281 (PVP01\_1211900) and a homologue of the *Drosophila* zinc-binding protein ‘Yippee’  
282 (PVP01\_0724100). Thrombospondin-1 like repeats (TSR: PF00090) and von Willebrand  
283 factor type A domains (PF00092) are enriched in sporozoites as well. In *P. falciparum*  
284 sporozoites, genes enriched in TSR domains are important in invasion of the mosquito  
285 salivary gland (e.g., *trap*) and secretory vesicles released by sporozoites upon entering the  
286 vertebrate host (e.g., *csp*) [42]. By comparison, genes up-regulated in blood-stages are  
287 enriched for *vir* gene domains (PF09687 and PF05796), Tryptophan-Threonine-rich  
288 *Plasmodium* antigens (PF12319; which are associated with merozoites [43]), markers of cell-  
289 division (PF02493; [44]) protein production/degradation (PF00112, PF10584, PF00152,  
290 PF09688 and PF00227) and ATP metabolism (PF08238 and PF12774). 47 of the 343  
291 transcripts unique to *P. vivax* sporozoites relative to *P. falciparum* or *P. yoelii* are up-  
292 regulated in sporozoites compared to *P. vivax* blood stages. Nine of these are in the top decile  
293 of transcription, and include a Pv-fam-e (PVP01\_0525200), a Pf-fam-b homolog  
294 (PVP01\_0602000) and 7 proteins of unknown function. A further nine have an ortholog in *P.*  
295 *cynomolgi* (which also forms hypnozoites) but not the closely related *P. knowlesi* (which does  
296 not form hypnozoites) and include ‘*msp7*’-like (PVP01\_1219600, PVP01\_1220300 and  
297 PVP01\_1219900), ‘*msp3*’-like (PVP01\_1031300), Pv-fam-e genes (PVP01\_0302100,  
298 PVP01\_0524500 and PVP01\_0523400), a serine-threonine protein kinase (PVP01\_0207300)  
299 and a RecQ1 helicase homolog (PVP01\_0717000). Notably, the *P. cynomolgi* ortholog of  
300 PVP01\_0207300, PCYB\_021650, is transcriptionally up-regulated in hypnozoites relative to  
301 replicating schizonts [23], indicating a target of significant interest when considering  
302 hypnozoite formation and/or biology and suggesting that the list here may contain other genes  
303 important in hypnozoite biology.

304  
305 **P. vivax sporozoites are enriched in translational repressors.** In *Plasmodium*, translational  
306 repression regulates key life-cycle transitions coinciding with switching between the  
307 mosquito and the mammalian host (either as sporozoites or gametocytes) [41]. For example,  
308 although *uis4* is the most abundant transcript in the infectious sporozoite ([24, 31]; Table S2),  
309 UIS4 is translationally repressed in this stage [15] and only expressed after hepatocyte  
310 invasion [45]. In sporozoites, it is thought that PUF2 binds to mRNA transcripts and prevents  
311 their translation [29], and SAPI stabilises the repressed transcripts and prevents their  
312 degradation [45]. Consistent with this, *Puf2* and *SAPI* (PVP01\_0947600) are up-regulated in  
313 the sporozoite relative to blood-stages. Indeed, *Puf2* (PVP01\_0526500) is among the top  
314 percentile of transcripts in salivary sporozoites and expressed at high levels in the proteome  
315 [33]. However, our data implicate other genes that may act in translational repression in *P.*  
316 *vivax* sporozoites, many of which are already known to be involved in translational repression  
317 in other *Plasmodium* stages and other protists [41]. Among these are *alba-2* and *alba-4*, both  
318 of which are among the top 2% of genes transcribed in sporozoites and ~14 to 20-fold more  
319 highly transcribed in sporozoites relative to blood-stages; ALBA-2 is in the top 100 most  
320 abundant proteins in the *P. vivax* sporozoite proteome [33]. In addition, *P. vivax* sporozoites  
321 are enriched for genes encoding RRM-6 RNA helicase domains. Intriguing among these are  
322 HoMu (homolog of Musashi; top decile of sporozoite proteins by abundance [33]) and *ptbp*  
323 (polypyrimidine tract binding protein). Musashi regulates eukaryotic stem cell differentiation  
324 through translational repression [46] and HoMu localizes with DOZI and CITH in  
325 *Plasmodium* gametocytes [47]. PTBP is linked to mRNA stability, splice regulation and  
326 translational initiation [48] and may perform a complementary role to SAPI.

327  
328 **P. vivax sporozoite relative to Plasmodium spp. liver stage transcriptomes.** New advances in  
329 *P. vivax* liver culture has allowed recent publication of mixed stage and hypnozoite-enriched  
330 transcriptomes [22]. This is an early, yet highly valuable, study and, due no doubt to the  
331 difficulty in generating the material, is limited to biological duplicates. Noting this, although  
332 we undertake differential transcriptomic studies of this dataset here, we recognize that  
333 additional biological replication is needed and have used a higher burden of significance

334 (FDR  $\leq 0.01$  and  $\geq 2$ -fold change) than used with blood-stages. Nevertheless, these  
335 comparisons identified 1,015 and 856 sporozoite up-regulated transcripts relative to mLS and  
336 HPZs respectively and 1,007 and 1,079 transcripts up-regulated in mLS and HPZs relative to  
337 sporozoites respectively (Figures 3 and S11-S13, Table S12 and S13 and Interactive Glimma  
338 Plot - Supplementary Data 1).

339 Compared to mLS transcriptomes, sporozoites are enriched for many of the  
340 transcripts similarly up-regulated in comparison to blood-stages (e.g., *uis4*, *celtos*, *puf2*, *siap1*  
341 and *plp-1*). More broadly, SPZ up-regulated transcripts over-represent (p-value  $\leq 0.05$ ) Pfam  
342 domains (Figure 3A) associated with transcriptional regulation (PF00176, PF01096, PF01661  
343 and PF08711), translational repression/regulation (PF00076, PF00279, PF01008, PF01873,  
344 PF01917, PF02847, PF02854, PF13893 and PF14259), DNA/RNA binding (PF0097,  
345 PF13445, PF13639, PF14570 and PF15247) and chromatin regulation (PF00271, PF00850  
346 and PF13489). In contrast, the mLS transcriptome is enriched in genes involved in replication  
347 and merozoite formation [n = 14; including PVP01\_0728900 (*mSP1*), PVP01\_0010670  
348 (*mSP3*) and PVP01\_1446800 (*mSP9*)], rho-try function [n = 9; including PVP01\_1469200  
349 (*rnp3*), PVP01\_1255000 (*rnp2*) and PVP01\_1338500 (*rap1*)] and reticulocyte binding [n=10  
350 including PVP01\_0534300 (*rbp2c*), PVP01\_1402400 (*rbp2a*), PVP01\_0701100 (*rbp1b*) and  
351 PVP01\_0800700 (*rbp2b*)]. These data are further enriched for Pfam domains associated with  
352 cell division (PF00493), merozoite formation (PF07133 and PF12984), proteasome function  
353 (PF00227, PF00400, PF00656, PF01344, PF01398 and PF03981), protein export / vesicle  
354 function (PF00350 and PF00996), membrane proteins (PF01105, PF03011, PF05424 and  
355 PF12139) and metabolism (PF00085, PF00118, PF00268, PF01066, PF01214 and PF01214).  
356 Collectively, in addition to markers consistent with sporozoite or merozoite formation, these  
357 data point towards the sporozoite stage as being highly regulated and controlled at  
358 transcriptional, translational and chromatin levels, with the mLS stages representing a release  
359 of this control allowing replication, protein turn-over, reconfiguration of the proteins on the  
360 plasma membrane and metabolic activity.

361 Comparison of sporozoites with HPZs does not indicate a similar release of control,  
362 or at least that any release is more specific than for mLS. The sporozoite is enriched, relative  
363 to HPZs, in genes such as PVP01\_1258000 (*gest*), PVP01\_0418000 (*sera*), PVP01\_1435400  
364 (*celtos*), PVP01\_0835600 (*csp*) and PVP01\_0602100 (*uis4*). At a broad level, sporozoite  
365 enriched Pfam domains include a smaller number associated with translational  
366 repression/regulation (PF00076) or DNA/RNA binding (PF01428 and PF12756).  
367 Interestingly, sporozoites are enriched in Pfam domains specifically associated with  
368 heterochromatin (H3K9me3) reading/interaction (PF02463, PF00628, PF13831 and  
369 PF13865). Ours (see below) and previous epigenetic studies of *Plasmodium* sporozoites [27]  
370 find dense heterochromatin in the telomeric to subtelomeric regions of the chromosome,  
371 which is more transcriptionally active in blood-stages [49]. Others have noted an up-  
372 regulation of methyl/acetyltransferases in *P. cynomolgi* HPZs [23] and/or shown  
373 methyltransferase inhibitors stimulate hypnozoite activation *in vitro* [17]. The potential that  
374 histone epigenetics of sporozoites has a role in or changes with liver-stage development and  
375 the formation of liver schizonts or HPZs is intriguing but requires detailed study of the  
376 chromatin of liver-stage parasites, which is not presently available for *P. vivax*. In contrast,  
377 HPZs were enriched, relative to sporozoites, for genes including histone proteins  
378 (PVP01\_1138700, PVP01\_1131700 and PVP01\_0905900) and classic markers of metabolism  
379 (PVP01\_MITO3300 and PVP01\_MITO3400) and *lisp2*. Pfam data indicated- largely similar  
380 domain enrichment trends as were seen for the mLS stage relative to sporozoites, including a  
381 number of proteosomal (PF00227, PF00112, PF03981), vesicular transport (PF00996) and  
382 metabolic (PF00118, PF00268, PF01066, PF01214 a) associated functions. This supports  
383 HPZs being an arrested, rather than classically 'dormant', stage with active metabolism and  
384 protein turn-over. HPZs are also enriched for Pfams associated with mRNA/tRNA regulation  
385 and turnover (PF04857, PF01612, PF00009 and PF01138) and glycine metabolism (PF01571  
386 and PF00464) and acetyl-CoA production (PF02779 and PF00676).

387 Finally, although not the focus of this study, we looked at differential transcription  
388 between mLS and HPZ stages using the Gural et al [22] data, but using the same approaches

389 as employed here. In particular, we were interested in what these comparisons might provide  
390 in terms of sporozoite differentiation or development into liver schizonts or HPZs (Table  
391 S14). Among mLS up-regulated transcripts are genes associated with rhoptry function (n =  
392 11; including PVP01\_0107500, PVP01\_1469200 and PVP01\_1469200), cytoadherence to  
393 red-cells (PVP01\_1401400 and PVP01\_0734500), merozoite formation (PVP01\_0728900  
394 and PVP01\_0612400) and exported proteins (n = 6; including PVP01\_0504000,  
395 PVP01\_0119200 and PVP01\_0801600). Consistent with *P. cynomolgi* [23], HPZ up-  
396 regulated transcripts include several key sporozoite transcripts, specifically *uis4*  
397 (PVP01\_0602100), *puf1* (PVP01\_1015000) and *speld* (PVP01\_0938800). At the Pfam  
398 domain level, mLS is enriched for metabolic (PF00317) and proteosomal (PF00112) domains  
399 also enriched in mLS or HPZs relative to sporozoites above, as well as domains associated  
400 with merozoite formation (PF12948, PF07462), rhoptry function (PF0712), DNA/RNA  
401 binding (PF12756, PF10601 and PF02151) and cell division, development and DNA  
402 replication (PF06705, PF00533, PF00488, PF02460, PF07034, PF02181). In contrast, HPZs  
403 are enriched in Pfam domains that overlap notably with key sporozoite markers, including  
404 *etramps* (PF09716) and *puf* proteins (PF00806), as well as domains associated with calcium  
405 (PF08683) and nucleotide metabolism (PF06437). These data largely indicate that the  
406 hypnozoite bears similarity both to the sporozoite and liver schizonts consistent with a stalled  
407 stage on the path to schizont development regulated by checkpoint signals that halt/restart  
408 normal schizont development, which has been proposed previously for this species [24].

409 With this in mind, we looked at transcripts that are differentially transcribed in mLS,  
410 but not HPZs, relative to SPZs. There are 107 transcripts down-regulated in mLS relative to  
411 SPZs that are transcribed at roughly similar levels in both SPZs and HPZs (Figure 3B). A  
412 common theme among many of these genes are their role in transcriptional, post-  
413 transcriptional, translational or post-translational regulation. Among transcriptional regulators  
414 are transcription factors including AP2-SP2 (PVP01\_0303400) and three non-AP2-like  
415 transcription factors (PVP01\_0306600, PVP01\_0204300 and PVP01\_1415800). Post-  
416 transcriptional controllers include several DNA/RNA-binding proteins (PVP01\_1011000,  
417 PVP01\_0932900, PVP01\_0715300, PVP\_1242600 and PVP01\_0605200), RNA helicases  
418 (PVP01\_1403600 and PVP01\_1329800) and mRNA processing (PVP01\_1443100 and  
419 PVP01\_1458200) genes. Translational control includes several key regulators of translation  
420 initiation (PVP01\_1467700), tRNA processing (PVP01\_0318700 and PVP01\_1017700) or  
421 ribosomal function/biogenesis (PVP01\_1443700, PVP01\_0421400, PVP01\_1117200 and  
422 PVP01\_0215100). Post-translational control includes two methyltransferases  
423 (PVP01\_1428800 and PVP01\_1465200), including CARM1, which methylates of H3R17  
424 and, in mice, prevents differentiation in embryonic stem cells [50], and a putative histone  
425 methylation reading enzyme, EEML2 (PVP01\_1014100). The remaining genes in this group  
426 have three noteworthy and largely overlapping themes: (1) an association with calcium  
427 binding, metabolism or signalling, (2) a role in organellar metabolism and (3) homologs in  
428 other organisms, including a variety of prokaryotes and eukaryotes, with key roles in  
429 germination, dormancy and persistent non-replicating stages. The latter most function is  
430 clearly intriguing in the context of HPZ formation and activation. These genes include a  
431 homolog of dihydrolipoamide acyltransferase (aka 'sucB'), which is essential for growth in  
432 *Mycobacterium tuberculosis* [51] and a key regulator in persistent *Escherichia coli* stages  
433 [52]. Another example is gamete fusion factor HAP2, which, despite the name, has been  
434 shown to regulate dormancy in eukaryotes ranging from plants [53, 54] to amoebae [55].

435 In addition to data for *P. vivax*, two transcriptomic studies are now available for *P.*  
436 *cynomolgi* [27, 56] that compare mixed/schizont stage parasites with small-form  
437 "hypnozoites". In comparing *P. cynomolgi* liver-stage RNA-seq and *P. vivax* liver-stage  
438 microarray data, Cubi et al [23] noted a moderate to good level of agreement ( $R^2 = 0.50$ ) as  
439 evidence of *P. cynomolgi* being predictive and representative of *P. vivax*. However, Voorberg  
440 van der Wel et al [56] explored congruence between their and the Cubi et al [23] studies and  
441 found generally good agreement among schizonts and overall relatively poor agreement  
442 among hypnozoites from each study. This highlights the complexity of these datasets and  
443 indicates caution in comparing the current data to *P. vivax*. ApiAP2 transcription factors



444 feature prominently in each liver-stage transcriptomic study for *P. cynomolgi* [23, 56] and *P.*  
445 *vivax* [22]. Cubi et al [23] noted an ApiAP2 (dubbed “AP2-Q”; PCYB\_102390) as  
446 transcriptionally up-regulated in *P. cynomolgi* hypnozoites and proposed this as a potential  
447 hypnozoite marker. We note that the *P. vivax* ortholog of *Pc*-AP2-Q (PVP01\_1016100) is  
448 among the genes detectable as a transcript but not protein in *P. vivax* sporozoites. This may  
449 point to a translationally repressed signal in sporozoites to regulate hypnozoite formation.  
450 However, as *Pv*-AP2-Q is transcribed at an abundance (~50 TPM) at or below which ~50% of  
451 *P. vivax* genes are detectable as transcripts but not as proteins (Figure 1B), this could as likely  
452 result from LC-MS detection sensitivity. Further, although AP2-Q was reported as specific to  
453 hypnozoite forming *Plasmodium* species [23], it is indeed found in non-hypnozoite producing  
454 species, such as *P. knowlesi*, *P. gallinaceum* and *P. inui* [56]. Up-regulation of AP2-Q  
455 transcripts is not observed for hypnozoites in subsequent transcriptomic studies of *P.*  
456 *cynomolgi* [56] or *P. vivax* [22], nor do we see such an up-regulation here. Voorberg van der  
457 Wel et al [56] note transcription of a range of AP2s in *P. cynomolgi* liver stages, but do not  
458 find any to be up-regulated in hypnozoites. AP2s also feature among transcribed genes in *P.*  
459 *vivax* liver stages, with one, PVP01\_0916300, significantly up-regulated in hypnozoites. We  
460 note that PVP01\_0916300 is up-regulated in *P. vivax* sporozoites relative to blood-stages and  
461 found in the top quartile of transcripts by abundance (TPM = 104).

462  
463 **Chromatin epigenetics in *P. vivax* sporozoites.** As noted above, transcriptomic data for  
464 sporozoites, and their comparison with liver and blood-stages, implicate histone epigenetics  
465 as having an important role in sporozoite biology and liver stage differentiation. This concept  
466 has been alluded to in recent liver-stage studies of *P. cynomolgi* [17, 23] that propose  
467 methyltransferases as having a potential role in hypnozoite formation. No epigenetic data are  
468 currently available for any *P. vivax* life-cycle stage. Studies of *P. falciparum* blood-stages  
469 have identified the importance of histone modifications as a primary epigenetic regulator [57,  
470 58] and characterized key markers of heterochromatin (H3K9me3) and  
471 euchromatin/transcriptional activation (H3K4me3 and H3K9ac). Recently, these marks have  
472 been explored with the maturation of *P. falciparum* sporozoites in the mosquito [26]. Here,  
473 we characterize major histone marks in *P. vivax* sporozoites and assess their relationship to  
474 transcript abundance.

475  
476 **Histone modifications in *P. vivax* sporozoites.** Using ChIP-seq, we identified 1,506, 1,999  
477 and 5,262 ChIP-seq peaks stably represented in multiple *P. vivax* sporozoite replicates and  
478 associated with H3K9me3, H3K9ac and H3K4me3 histone marks respectively (Figure 4 and  
479 S14-S19). Peak width, spacing and stability differed with histone mark type (Figures S15 and  
480 S16). H3K4me3 covered the greatest breadth of the genome (36.0% of all bases) and was the  
481 most stable among replicates, with ~84% of bases associated with an H3K4me3 found in  
482 multiple biological replicates. By comparison H3K9me3 marks were least stable, with 46% of  
483 bases associated with this mark found in just one replicate. Consistent with observations in *P.*  
484 *falciparum*, H3K9me3 ‘heterochromatin’ marks primarily clustered in telomeric and  
485 subtelomeric regions (Figure 4). In contrast, the ‘euchromatin’ / transcriptionally open  
486 histone marks, H3K4me3 and H3K9ac, were distributed in chromosome central regions and  
487 did not overlap with regions under H3K9me3 suppression. Both H3K9me3 and H3K4me3  
488 marks were reasonably uniformly distributed (mean peak spacing ~500bp for each) within  
489 their respective regions of the genome. In contrast, H3K9ac peaks were spaced further apart  
490 (mean: ~2kb), but also with a greater variability in spacing (likely reflecting their association  
491 with promoter regions [59]; Figure S17 and S19). The instability of H3K9me3 may reflect its  
492 use in *Plasmodium* for regulating expression of contingency genes from multigene families,  
493 whose members have overlapping and redundant functions [49] and confer phenotypic  
494 plasticity [60].

495  
496 **Genes under histone regulation.** We explored an association between these histone marks  
497 and the transcriptional behaviour of protein coding genes (Figure 4 and S19 and Tables S15-  
498 S20). 485 coding genes stably intersected with an H3K9me3 mark; all are located near the

499 ends of the chromosomal scaffolds (i.e., are (sub)telomeric). On average, these genes are  
500 transcribed at ~30 fold lower levels (mean 0.7 TPM) than genes not stably intersected by  
501 H3K9me3 marks. These data clearly support the function of this mark in transcriptional  
502 silencing. This is largely consistent with observations in *P. falciparum* sporozoites [26],  
503 however, in contrast to *P. falciparum* sporozoites where a single *var* gene was described to  
504 lack heterochromatin structure [27] we observe no genes within heterochromatin dense region  
505 that lacked a stable H3K9me3 signal or were transcribed at notable levels (i.e., above ~5  
506 TPM). Whether this relates to differences in epigenetic control between the species is not  
507 clear. We note that (sub)telomeric genes are overall transcriptionally silent in *P. vivax*  
508 sporozoites relative to blood-stages (Figure 4 and Tables S21 and S22). Consistent with  
509 observations in *P. falciparum* [57], the bulk of these genes include complex protein families,  
510 such as *vir* and *Pv-fam* genes, which are so far described to function primarily in blood-  
511 stages. Also notable among the genes are several reticulocyte-binding proteins, including  
512 RBP2, 2a, 2b and 2c. This transcriptional silence in telomeric and subtelomeric regions was  
513 recently observed in *P. falciparum* sporozoites [27].

514 Outside of the telomeres and subtelomeres, H3K4me3 marks are stably associated  
515 with the intergenic regions of 3,676 genes. H3K9ac marks are also identified within 1kb of  
516 the transcriptional start site (TSS) of 1,284 coding genes, with 1085 of these stably marked  
517 also by H3K4me3 (Figure 4B). The average transcription of these genes is 50, 112 and 112  
518 TPMs respectively (72, 160 and 160-fold higher than H3K9me3 marked genes). Gene-by-  
519 gene observations show that H3K9ac and H3K4me3 marks cluster densely in the 1000kb up  
520 and down-stream of the start and stop codon respectively of transcribed genes, but are much  
521 less dense within coding regions of these genes (Figure S15). This pattern directly correlates  
522 with transcription and contrasts H3K9me3 marks, which are distributed across the length of  
523 the gene at even density and are correlated with a lack of transcription. These data support the  
524 role of H3K9ac and H3K4me3 in transcriptional activation in *P. vivax*. The lower  
525 transcriptional abundance of H3K4me3 marked, compared with H3K9ac or H3K9ac and  
526 H3K4me3 marked genes suggest these marks work synergistically and that H3K9ac is  
527 possibly the better of the two, as a single mark indicator of transcriptional activity in *P. vivax*.  
528 This is consistent with recent observations in *P. falciparum* sporozoites [26].

529 Interestingly, H3K9ac-marked genes ranged in transcriptional activity from the most  
530 abundantly transcribed genes to many in the lower 50% and even lowest decile of  
531 transcription. This suggests more contributes to transcriptional activation in *P. vivax*  
532 sporozoites than, simply, gene accessibility through chromatin regulation. Specific activation  
533 by a transcription factor (e.g., ApiAP2s [61]) is the obvious candidate. To explore this, we  
534 compared upstream regions (within 1kb of the TSS or up to the 3' end of the next gene  
535 upstream, whichever was less) of highly (top 10%) and lowly (bottom 10%) transcribed  
536 H3K9ac marked genes for over-represented sequence motifs in the highly expressed genes  
537 that might coincide with known ApiAP2 transcription factor binding sites [62]. We identified  
538 these based on the location of the nearest stable H3K9ac peak relative to the transcription  
539 start site for each gene (Figure S12). In most instances, these peaks were within 100bp of the  
540 TSS and, consistent with data from *P. falciparum* [59], *P. vivax* promoters appear to be no  
541 more than a few hundred to a maximum of 1000 bp upstream of the TSS. Exploring these  
542 regions, we identified two over-represented motifs: TGTACMA (e-value  $2.7e^{-2}$ ) and  
543 ATATTTTH (e-value  $3.3e^{-3}$ ) (Fig. 2D). TGTAC is consistent with the known binding site for  
544 *Pf*-AP2-G, which regulates sexual differentiation in gametocytes [63], but its *P. vivax*  
545 ortholog (PVP01\_1418100) is neither highly transcribed nor expressed in sporozoites.  
546 ATATTTTH is similar to the binding motif for *Pf*-AP2-L (AATTTCC), a transcription factor  
547 that is important for liver stage development in *P. berghei* [64]. In contrast to AP2-G, *Pv*-  
548 AP2-L (PVX\_081180) is in the top 10% of transcription and expression in *P. vivax*  
549 sporozoites and up-regulated relative to blood-stages. In *P. vivax* sporozoites, the ATATTTTH  
550 motif is associated with a number of highly transcribed genes, including *lisp1* and *uis2-4*,  
551 known to be regulated by AP2-L in *P. berghei* [64] as well as many of the most highly  
552 transcribed, H3K9ac marked genes, including two *etramps* (PVP01\_0734800 and  
553 PVP01\_0504800), several RNA-binding proteins, including *Puf2*, *ddx5*, a putative ATP-

554 dependent RNA helicase DBP1 (PVP01\_1429700), and a putative *bax1* inhibitor  
555 (PVP01\_1465600). Interestingly, a number of highly transcribed and translationally repressed  
556 genes associated with the ATATTTTH motif, including *uis4*, *siap2* and *pv1*, are not stably  
557 marked by H3K9ac in all replicates (i.e., there is significant variation in the placement of the  
558 H3K9ac peak or their presence/absence among replicates for these genes). It may be that  
559 additional histone modifications, for example H3K27me, H3R17me3 or H2A or H4  
560 modifications, are involved in regulating transcription of these genes. Certainly the  
561 incorporation of the H2A.Z histone variant, which is present in intergenic regions of *P.*  
562 *falciparum* (Petter et al 2011), and controls temperature responses in plants [65] is intriguing  
563 as a potential mark regulating sporozoite fate in *P. vivax* considering the association between  
564 hypnozoite activation rate and climate [11], as is H3R17me3 in consideration of the  
565 enrichment of markers/readers of this modification in HPZs noted above and the role of this  
566 mark in cell fate progression in other species [50].

567

## 568 CONCLUSIONS

569 We provide the first comprehensive study of the transcriptome and epigenome of mature  
570 *Plasmodium vivax* sporozoites and undertake detailed comparisons with recently published  
571 proteomic data for *P. vivax* sporozoites [33] and transcriptomic data for *P. vivax* mixed and  
572 hypnozoite-enriched liver-stages [22] and mixed blood-stages [40]. These data support the  
573 proposal that the sporozoite is a highly-programmed stage that is primed for invasion of and  
574 development in the host hepatocyte. Cellular regulation, including at transcription,  
575 translational and epigenetic levels, appears to play a major role in shaping this stage (which  
576 continues on in some form in hypnozoites), and many of the genes proposed here as being  
577 under translational repression are involved in hepatocyte infection and early liver-stage  
578 development (Figure 5). We highlight a major role for RNA-binding proteins, including  
579 PUF2, ALBA2/4 and, intriguingly, ‘Homologue of Musashi’ (HoMu). We find that  
580 transcriptionally, the hypnozoite appears to be a transition point between the sporozoite and  
581 replicating schizonts, having many of the dominant sporozoite transcripts and retaining high  
582 transcription of a number of key regulatory pathways involved in transcription, translation  
583 and chromatin configuration (including histone arginine methylation). A consistent theme in  
584 the study is the prominence of a number of genes that have a role in numerous eukaryotic  
585 systems in cell fate determination and differentiation (e.g., HoMu, Yippee and CARM1) and  
586 overlap with dormancy and/or persistent cell states in bacteria, protists or higher eukaryotes  
587 (e.g., bacterial *sucB* and gamete fusion protein HAP2). These data do not point to one single  
588 programming switch for dormancy or liver developmental fate in *P. vivax*, but present a  
589 number of intriguing avenues for exploration in subsequent studies, particularly in model  
590 species such as *P. cynomolgi*. Our study contributes to understanding the early stages of  
591 hepatocyte infection and the developmental switch between liver trophozoite and hypnozoite  
592 formation. We also identify potential avenues for rationally prioritizing targets underpinning  
593 liver-stage differentiation for functional evaluation in humanized mouse and simian models  
594 for relapsing *Plasmodium* species and identifying novel avenues to understand and eradicate  
595 liver-stage infections.

596

## 597 MATERIALS AND METHODS

598 **Ethics Statement.** Collection of venous blood from human patients with naturally acquired  
599 vivax infection for the current study was approved by the Ethical Review Committee of the  
600 Faculty of Tropical Medicine, Mahidol University (Human Subjects Protocol number TMEC  
601 11-033) with the informed written consent of each donor individual. All mouse tissue used in  
602 the current study was from preserved infected tissues generated previously [13]. All mouse  
603 infection work in [13] was carried out at the Centre for Infectious Diseases Research (CIDR)  
604 in Seattle, USA, under direct approval of the CIDR Institutional Animal Care and Use  
605 Committee (IACUC) and performed in strict accordance with the recommendations in the  
606 Guide for the Care and Use of Laboratory Animals of the National Institutes of Health, USA.  
607 The Centre for Infectious Disease Research Biomedical Research Institute has an Assurance

608 from the Public Health Service (PHS Assurance number is A3640-01) through the Office of  
609 Laboratory Animal Welfare (OLAW) for work approved by its IACUC.

610

611 **Material collection, isolation and preparation.** Nine field isolates (PvSpz-Thai 1 to 9),  
612 representing symptomatic blood-stage malaria infections were collected as venous blood (20  
613 mL) from patients presenting at malaria clinics in Tak and Ubon Ratchatani provinces in  
614 Thailand. Each isolate was used to establish, infections in *Anopheles dirus* colonized at  
615 Mahidol University (Bangkok) by membrane feeding [13], after 14-16 days post blood  
616 feeding, ~3-15 million sporozoites were harvested per field isolate from the salivary glands of  
617 up to 1,000 of these mosquitoes as per [66] and shipped in preservative (trizol (RNA/DNA) or  
618 1% paraformaldehyde (DNA for ChIP-seq) to the Walter and Eliza Hall Institute (WEHI).

619

620 **Transcriptomics sequencing and differential analysis.** Upon arrival at WEHI, messenger  
621 RNAs were purified from an aliquot (~0.5-1 million sporozoites) of each *P. vivax* field isolate  
622 as per [40] and subjected to RNA-seq on Illumina NextSeq using TruSeq library construction  
623 chemistry as per the manufacturer's instructions. Raw reads for each RNA-seq replicate are  
624 available through the Sequence Read Archive (XXX-XXX). Sequencing adaptors were  
625 removed and low quality reads trimmed and filtered using Trimmomatic v. 0.36 [67]. To  
626 remove host contaminants, processed reads were aligned, as single-end reads, to the  
627 *Anopheles dirus* wrari2 genome (VectorBase version W1) using Bowtie2 [68] (--very-  
628 sensitive preset). All non-host reads were then aligned to the manually curated transcripts of  
629 the *P. vivax* P01 genome (<http://www.genedb.org/Homepage/PvivaxP01>; [28]) using RSEM  
630 [69] (pertinent settings: --bowtie2 --bowtie2-sensitivity-level very\_sensitive --calc-ci --ci-  
631 memory 10240 --estimate-rspd --paired-end). Transcript abundance for each gene in each  
632 replicate was calculated by RSEM as raw count, posterior mean estimate expected counts  
633 (pme-EC) and transcripts per million (TPM).

634

635 Transcriptional abundance in *P. vivax* sporozoites was compared qualitatively (by  
636 ranked abundance) with previously published microarray data for *P. vivax* salivary-gland  
637 sporozoites [24]. As a further quality control, these RNA-seq data were compared also with  
638 previously published microarray data for *P. falciparum* salivary-gland sporozoites [30], as  
639 well as RNA-seq data from salivary-gland sporozoites generated here for *P. falciparum*  
640 (single replicate generated from *P. falciparum* 3D7 lab cultures isolated from *Anopheles*  
641 *stephensi* and processed as above) and previously published for *P. yoelii* [29]. RNA-seq data  
642 from these additional *Plasmodium* species were (re)analysed from raw reads and  
643 transcriptional abundance for each species was determined (raw counts and pme-EC and TPM  
644 data) as described above using gene models current as of 04-10-2016 (PlasmoDB release  
645 v29). Interspecific transcriptional behaviour was qualitatively compared by relative ranked  
646 abundance in each species using TPM data for single copy orthologs (SCOs; defined in  
647 PlasmoDB) only, shared between *P. vivax* and *P. falciparum* or shared among *P. vivax*, *P.*

648

649 *falciparum* and *P. yoelii*.  
650 To define transcripts that were up-regulated in sporozoites, we remapped raw reads  
651 representing early (18-24 hours post-infection (HPI)), mid (30-40 HPI) and late (42-46 HPI)  
652 *P. vivax* blood-stage infections recently published by Zhu *et al* [40] to the *P. vivax* P01  
653 transcripts using RSEM as above. All replicate data was assessed for mapping metrics,  
654 transcript saturation and other standard QC metrics using QualiMap v 2.1.3 [70]. Differential  
655 transcription between *P. vivax* salivary-gland sporozoites and mixed blood-stages [40] was  
656 assessed using pme-EC data in EdgeR [71] and limma [72] (differential transcription cut-off:  
657  $\geq 2$ -fold change in counts per million (CPM) and a False Discovery Rate (FDR)  $\leq 0.05$ ).  
658 Pearson Chi squared tests were used to detect over-represented Pfam domains and Gene  
659 Ontology (GO) terms among differentially transcribed genes in sporozoites (Bonferroni-  
660 corrected  $p < 0.05$ ), based on gene annotations in PlasmoDB (release v29).

661

662 We also compared transcription of the sporozoite stages to recently published liver-  
663 stage data from Gural *et al* [22] as per the sporozoite to blood-stage comparisons above, with  
664 the following modifications: (1) EC values were normalized using the 'upper quartile' method  
665 instead of TMM, (2) differential transcription was assessed using a quasi-likelihood

663 generalize linear model (instead of a linear model) and (3) an FDR threshold for significance  
664 of  $\leq 0.01$  was used instead of  $\leq 0.05$ . These differences related to specific attributes of the  
665 liver-stage dataset, particularly the small number of replicates ( $n = 2$ ) per experiment  
666 condition. Data visualization and interactive R-shiny plots were produced in R using the  
667 ggplot[73], ggplot2 [74], gplots(heatmap.2) [75] and Glimma [76] packages.

668  
669 **Assessment of Sporozoite RNA-seq transcriptome by selective RT-qPCR:** Extracted RNA  
670 was DNase treated (Sigma D5307) as per manufacturer recommendations. RNA was  
671 quantified using the TapeStation High Sensitivity RNA kit (Agilent). Two intron-spanning  
672 primer pairs were designed per gene of interest using Primer3 and BLAST. Primer pairs were  
673 tested in two concentrations (0.75ng and 2.83ng per reaction) to determine efficiency and  
674 specificity. Product was run on a 1% agarose gel with ethidium bromide. Primer pairs  
675 indicating non-specific priming were removed. The resulting 11 primer pairs were used on  
676 four sporozoite samples; VUBR06, VUNL23, VUBR24, VTTY84. RNA was reverse  
677 transcribed (Sensifast, Bioline) and used at 0.75ng per reaction, run on a Roche LightCycler  
678 480 II. Melt curves were assessed and products were run on a gel to ensure specificity again.  
679 Cp threshold was set automatically.  $\Delta C_p$  value was calculated as target gene – comparator  
680 gene (SERA and CelTOS were used). Data were log transformed and fold change calculated.

681  
682 RT-qPCR Primers were as follows:

Name	Gene	Forward Primer	Reverse Primer
RPS27	PVX_122245	ACCACCTTGTTTAGCCATGC	TAATTTGCACTTCCACCCGTT
D13	PVX_089510	CTGTACACGCACGAGCTGGC	CAGCTCCTTGACGCCACTG
G10	PVX_080110	ACGAGCTGTACTACAAGCGGA	TTTCTCCTGCACCAGGTAGTC
AP2	PVX_086995*	GCCCCACTGGAAGTTTTGGA	CGTTCAGCCGCTGGTAGTAT
SERA	PVX_003790	CTGAAGACCTCCAGGGACAAG	TTTCTGCCTCTCCAGTGATATCTTT
CelTOS	PVX_123510*	CCCCCAAAGGCAAAATGAACAA	CGCTCTTCCCCTCAAGGAC
GEST	PVX_118040	GACATATCAAGCAGTGAGGGA	CATGTTGTGGCCTTTATATGCTG
ALBA4	PVX_083270	TATCAACGGAGCCTTTGCCG	GGACTTGATTTCCCTCGTCGG
PUF2	PVX_089945	ATCATAGAGAACGTCGACAAGCTTA	CTACGTTTCCAGGTTGCTGATC
14-3-3	PVX_089505	GACAACCTGACCTGTGGACGTC	TACTCGAGGCCTTCATCCTTCGATT
ZIPCO	PVX_001980	TTAGCTCAATTGCTTGTGGCTTTT	TGCCACTAACTCCAAGGAAATAACT

683

684 \* denotes single exon gene

685

686 **Salivary-gland sporozoite and liver-stage immunofluorescence assays (IFAs).** IFAs were  
687 performed as per [13] using preserved, vivax infected mouse liver tissue generated previously  
688 for that study. In [13], female FRG [fumarylacetoacetate hydrolase (F), recombination  
689 activation gene 2 (R), interleukin-2 receptor subunit gamma (G)] triple KO mice engrafted  
690 with human hepatocytes (FRG KO huHep) were purchased from Yecuris Corporation  
691 (Oregon, USA). Mice were infected through intravenous injection into the tail with  $3.5 \times$   
692  $10^5$  to  $1 \times 10^6$  sporozoites isolated from the salivary glands of infected mosquitoes in 100  $\mu$ l  
693 of RPMI media. Liver stages for the current study were obtained from 10 $\mu$ m formalin fixed  
694 paraffin embedded day 7 liver stages generated previously [13] from FRG knockout huHep  
695 mice; [13] these were deparaffinized prior to staining. Fresh salivary-gland sporozoites were  
696 fixed in acetone per [13]. All cells were incubated twice for 3 minutes in Xylene, then 100%  
697 Ethanol, and finally once for 3 minutes each in 95%, 70%, and 50% Ethanol. The cells were  
698 rinsed in DI water and permeabilized immediately in 1XTBS, containing Triton X-100 and  
699 30% hydrogen peroxide. The cells were blocked in 5% milk in 1XTBS. The hepatocytes were  
700 stained overnight with a rabbit polyclonal LISP1 antibody (A), a rabbit polyclonal UIS4

701 antibody (B), and a rabbit polyclonal BIP antibody (C) in blocking buffer. The cells were  
702 washed with 1XTBS and the primary antibodies were detected with goat anti-rabbit Alexa  
703 Fluor 488 antibody (Life Technologies). The cells were washed in 1XTBS. The hepatocytes  
704 were rinsed in KMNO<sub>4</sub> and washed in 1XTBS. The cells were incubated in DAPI for 5  
705 minutes.

706  
707 **Histone ChIP sequencing and analysis.** Aliquots of 2 – 6 million freshly isolated  
708 sporozoites were fixed with 1% paraformaldehyde for 10 min at 37°C and the reaction  
709 subsequently quenched by adding glycine to a final concentration of 125 mM. After three  
710 washes with PBS, sporozoite pellets were stored at -80°C and shipped to Australia. Nuclei  
711 were released from the sporozoites by dounce homogenization in lysis buffer (10 mM Hepes  
712 pH 7.9, 10 mM KCl, 0.1 mM EDTA, 0.1 mM EDTA, 1 mM DTT, 1x EDTA-free protease  
713 inhibitor cocktail (Roche), 0.25% NP40). Nuclei were pelleted by centrifugation at 21,000 g  
714 for 10 min at 4°C and resuspended in SDS lysis buffer (1% SDS, 10 mM EDTA, 50 mM Tris  
715 pH 8.1, 1x EDTA-free protease inhibitor cocktail). Chromatin was sheared into 200–1000 bp  
716 fragments by sonication for 16 cycles in 30 sec intervals (on/off, high setting) using a  
717 Bioruptor (Diagenode) and diluted 1:10 in ChIP dilution buffer (0.01% SDS, 1.1% Triton X-  
718 100, 1.2 mM EDTA, 16.7 mM Tris pH 8.1, 150 mM NaCl). Chromatin was precleared for 1  
719 hour with protein A/G sepharose (4FastFlow, GE Healthcare) equilibrated in 0.1% BSA  
720 (Sigma-Aldrich, USA) in ChIP dilution buffer. Chromatin from 3 x 10<sup>5</sup> nuclei was taken  
721 aside as input material. Chromatin from approximately 3 x 10<sup>6</sup> sporozoite nuclei was used for  
722 each ChIP. ChIP was carried out over night at 4°C with 5 µg of antibody (H3K9me3 (Active  
723 Motif), H3K4me3 (Abcam), H3K9ac (Upstate), H4K16ac (Abcam)) and 10 µl each of  
724 equilibrated protein A and G sepharose beads (4FastFlow, GE Healthcare). After washes in  
725 low-salt, high-salt, LiCl, and TE buffers (EZ-ChIP Kit, Millipore), precipitated complexes  
726 were eluted in 1% SDS, 0.1 M NaHCO<sub>3</sub>. Cross-linking of the immune complexes and input  
727 material was reversed for 6 hours at 45°C after addition of 500 mM NaCl and 20 µg/ml of  
728 proteinase K (NEB). DNA was purified using the MinElute® PCR purification kit (Qiagen)  
729 and paired-end sequenced on Illumina NextSeq using TruSeq library construction chemistry  
730 as per the manufacturer's instructions. Raw reads for each ChIP-seq replicate are available  
731 through the Sequence Read Archive (XXX-XXX).

732 Fastq files were checked for quality using fastqc  
733 (<http://www.bioinformatics.babraham.ac.uk/projects/fastqc/>) and adapter sequences were  
734 trimmed using cutadapt [77]. Paired end reads were mapped to the *P. vivax* P01 strain  
735 genome annotation using Bowtie2 [68]. The alignment files were converted to Bam format,  
736 sorted and indexed using Samtools [78]. ChIP peaks were called relative to input using  
737 MACS2[79] in paired end mode with a q value less than or equal to 0.01. Peaks and peak  
738 summits were converted to sorted BED files. Bedtools intersect[80] was used to identify  
739 genes that intersected H3K9me3 peaks and Bedtools closest was used to identify genes that  
740 were closest to and downstream of H3K9ac and H3K4me3 peak summits.

741  
742 **Sequence motif analysis.** Conserved sequence motifs were identified using the program  
743 DREME [81]. Only genes in the top decile of transcription showing no evidence of protein  
744 expression in multiple salivary-gland sporozoite replicates were considered as putatively  
745 translationally repressed (n = 170). We queried coding regions and regions upstream of the  
746 transcriptional start site (TSS) for each gene, defined by Zhu *et al* [40] and/or predicted here  
747 from all RNA-seq data using the Tuxedo suite [82], for enriched sequence motifs in  
748 comparison to 170 genes found to be in the top decile of both transcriptional and expressional  
749 abundance in the same sporozoite replicates. In searching for motifs associated with highly  
750 transcribed genes with stable H3K9ac marks within 1kb of the TSS (or up to the 3' end of the  
751 next gene upstream), we compared H3K9ac marked genes in the top decile of transcription to  
752 the same number of H3K9ac marked genes in the bottom decile of transcription. In both  
753 instances, an e-value threshold of 0.05 was considered the minimum threshold for statistical  
754 significance.

755

756 **References**

- 757 1. Organization WH. World Malaria Report 2015. WHO, Geneva. 2015.
- 758 2. Feachem RG, Phillips AA, Hwang J, Cotter C, Wielgosz B, Greenwood BM, et al.  
759 Shrinking the malaria map: progress and prospects. *Lancet*. 2010;376  
760 9752:1566-78. doi:10.1016/S0140-6736(10)61270-6.
- 761 3. Price RN, Douglas NM and Anstey NM. New developments in *Plasmodium vivax*  
762 malaria: severe disease and the rise of chloroquine resistance. *Curr Opin Infect*  
763 *Dis*. 2009;22 5:430-5. doi:10.1097/QCO.0b013e32832f14c1.
- 764 4. Baird KJ. Malaria caused by *Plasmodium vivax*: recurrent, difficult to treat,  
765 disabling, and threatening to life - averting the infectious bite preempts these  
766 hazards. *Pathogens and global health*. 2013;107:475-9.
- 767 5. Sattabongkot J, Tsuboi T, Zollner GE, Sirichaisinthop J and Cui L. *Plasmodium*  
768 *vivax* transmission: chances for control? *Trends in parasitology*. 2004;20 4:192-  
769 8.
- 770 6. Mueller I, Galinski MR, Baird JK, Carlton JM, Kochar DK, Alonso PL, et al. Key gaps  
771 in the knowledge of *Plasmodium vivax*, a neglected human malaria parasite.  
772 *Lancet Infect Dis*. 2009;9 9:555-66.
- 773 7. Lindner SE, Miller JL and Kappe SH. Malaria parasite pre-erythrocytic infection:  
774 preparation meets opportunity. *Cell Microbiol*. 2012;14 3:316-24.
- 775 8. Shin SC, Vanderberg JP and Terzakis JA. Direct infection of hepatocytes by  
776 sporozoites of *Plasmodium berghei*. *J Protozool*. 1982;29 3:448-54.
- 777 9. Mota MM, Pradel G, Vanderberg JP, Hafalla JC, Frevert U, Nussenzweig RS, et al.  
778 Migration of *Plasmodium* sporozoites through cells before infection. *Science*.  
779 2001;291 5501:141-4.
- 780 10. Lysenko AJ, Beljaev A and Rybalka V. Population studies of *Plasmodium vivax*: 1.  
781 The theory of polymorphism of sporozoites and epidemiological phenomena of  
782 tertian malaria. *Bull WHO*. 1977;55 5:541.
- 783 11. White NJ. Determinants of relapse periodicity in *Plasmodium vivax* malaria.  
784 *Malar J*. 2011;10:297.
- 785 12. Price RN, Tjitra E, Guerra CA, Yeung S, White NJ and Anstey NM. Vivax malaria:  
786 neglected and not benign. *Amer J Trop Med Hyg*. 2007;77 6 Suppl:79-87.
- 787 13. Mikolajczak SA, Vaughan AM, Kangwanrangsan N, Roobsoong W, Fishbaugher M,  
788 Yimamnuaychok N, et al. *Plasmodium vivax* liver stage development and  
789 hypnozoite persistence in human liver-chimeric mice. *Cell Host Microbe*.  
790 2015;17 4:526-35.
- 791 14. Mueller A-K, Camargo N, Kaiser K, Andorfer C, Frevert U, Matuschewski K, et al.  
792 *Plasmodium* liver stage developmental arrest by depletion of a protein at the  
793 parasite-host interface. *Proc Nat'l Acad Sci USA*. 2005;102 8:3022-7.
- 794 15. Silvie O, Briquet S, Muller K, Manzoni G and Matuschewski K. Post-  
795 transcriptional silencing of UIS4 in *Plasmodium berghei* sporozoites is important  
796 for host switch. *Mol Microbiol*. 2014;91 6:1200-13.
- 797 16. Mackellar DC, O'Neill MT, Aly AS, Sacci JB, Jr., Cowman AF and Kappe SH.  
798 *Plasmodium falciparum* PF10\_0164 (ETRAPM10.3) is an essential  
799 parasitophorous vacuole and exported protein in blood stages. *Eukaryot Cell*.  
800 2010;9 5:784-94.
- 801 17. Demebele L, Franetich JF, Lorthois A, Gego A, Zeeman AM, Kocken CH, et al.  
802 Persistence and activation of malaria hypnozoites in long-term primary  
803 hepatocyte cultures. *Nat Med*. 2014;20 3:307-12.
- 804 18. Malmquist NA, Moss TA, Mecheri S, Scherf A and Fuchter MJ. Small-molecule  
805 histone methyltransferase inhibitors display rapid antimalarial activity against  
806 all blood stage forms in *Plasmodium falciparum*. *Proc Nat'l Acad Sci USA*.  
807 2012;109 41:16708-13.
- 808 19. Josling GA and Llinas M. Sexual development in *Plasmodium* parasites: knowing  
809 when it's time to commit. *Nat Rev Microbiol*. 2015;13 9:573-87.

- 810 20. White MT, Karl S, Battle KE, Hay SI, Mueller I and Ghani AC. Modelling the  
811 contribution of the hypnozoite reservoir to *Plasmodium vivax* transmission. *Elife*.  
812 2014;3.
- 813 21. Roobsoong W, Tharinjaroen CS, Rachaphaew N, Chobson P, Schofield L, Cui L, et  
814 al. Improvement of culture conditions for long-term in vitro culture of  
815 *Plasmodium vivax*. *Malaria J*. 2015;14 1:1.
- 816 22. Gural N, Mancio-Silva L, Miller AB, Galstian A, Butty VL, Levine SS, et al. In vitro  
817 culture, drug sensitivity, and transcriptome of *Plasmodium vivax* hypnozoites.  
818 *Cell Host Microbe*. 2018;23 3:395-406 e4.
- 819 23. Cubi R, Vembar SS, Biton A, Franetich JF, Bordessoulles M, Sossau D, et al. Laser  
820 capture microdissection enables transcriptomic analysis of dividing and  
821 quiescent liver stages of *Plasmodium* relapsing species. *Cell Microbiol*. 2017.
- 822 24. Westenberger SJ, McClean CM, Chattopadhyay R, Dharia NV, Carlton JM,  
823 Barnwell JW, et al. A systems-based analysis of *Plasmodium vivax* lifecycle  
824 transcription from human to mosquito. *PLoS Negl Trop Dis*. 2010;4 4:e653.
- 825 25. Kim A, Popovici J, Vantaux A, Samreth R, Bin S, Kim S, et al. Characterization of *P*.  
826 *vivax* blood stage transcriptomes from field isolates reveals similarities among  
827 infections and complex gene isoforms. *Sci Rep*. 2017;7 1:7761.
- 828 26. Gomez-Diaz E, Yerbanga RS, Lefevre T, Cohuet A, Rowley MJ, Ouedraogo JB, et al.  
829 Epigenetic regulation of *Plasmodium falciparum* clonally variant gene expression  
830 during development in *Anopheles gambiae*. *Sci Rep*. 2017;7:40655.
- 831 27. Zanghi G, Vembar SS, Baumgarten S, Ding S, Guizetti J, Bryant JM, et al. A specific  
832 PfEMP1 is expressed in *P. falciparum* sporozoites and plays a role in hepatocyte  
833 infection. *Cell Rep*. 2018;22 11:2951-63.
- 834 28. Auburn S, Bohme U, Steinbiss S, Trimarsanto H, Hostetler J, Sanders M, et al. A  
835 new *Plasmodium vivax* reference sequence with improved assembly of the  
836 subtelomeres reveals an abundance of pir genes. *Wellcome Open Res*. 2016;1:4.
- 837 29. Lindner SE, Mikolajczak SA, Vaughan AM, Moon W, Joyce BR, Sullivan WJ, Jr., et  
838 al. Perturbations of *Plasmodium* Puf2 expression and RNA-seq of Puf2-deficient  
839 sporozoites reveal a critical role in maintaining RNA homeostasis and parasite  
840 transmissibility. *Cell Microbiol*. 2013;15 7:1266-83.
- 841 30. Le Roch KG, Johnson JR, Florens L, Zhou Y, Santrosyan A, Grainger M, et al. Global  
842 analysis of transcript and protein levels across the *Plasmodium falciparum* life  
843 cycle. *Genome research*. 2004;14 11:2308-18.
- 844 31. Mikolajczak SA, Silva-Rivera H, Peng X, Tarun AS, Camargo N, Jacobs-Lorena V, et  
845 al. Distinct malaria parasite sporozoites reveal transcriptional changes that  
846 cause differential tissue infection competence in the mosquito vector and  
847 mammalian host. *Mol Cell Biol*. 2008;28 20:6196-207.
- 848 32. Carlton JM, Adams JH, Silva JC, Bidwell SL, Lorenzi H, Caler E, et al. Comparative  
849 genomics of the neglected human malaria parasite *Plasmodium vivax*. *Nature*.  
850 2008;455 7214:757-63.
- 851 33. Swearingen KE, Lindner SE, Flannery EL, Vaughan AM, Morrison RD,  
852 Patrapuvich R, et al. Proteogenomic analysis of the total and surface-exposed  
853 proteomes of *Plasmodium vivax* salivary gland sporozoites. *PLoS Negl Trop Dis*.  
854 2017;11 7:e0005791.
- 855 34. Guerreiro A, Deligianni E, Santos JM, Silva PA, Louis C, Pain A, et al. Genome-wide  
856 RIP-Chip analysis of translational repressor-bound mRNAs in the *Plasmodium*  
857 gametocyte. *Genome Biol*. 2014;15 11:493.
- 858 35. Silvie O, Briquet S, Müller K, Manzoni G and Matuschewski K.  
859 Post-transcriptional silencing of UIS4 in *Plasmodium berghei* sporozoites is  
860 important for host switch. *Molecular microbiology*. 2014;91 6:1200-13.
- 861 36. Lindner SE, Swearingen KE, Harupa A, Vaughan AM, Sinnis P, Moritz RL, et al.  
862 Total and putative surface proteomics of malaria parasite salivary gland  
863 sporozoites. *Mol Cell Proteomics : MCP*. 2013;12 5:1127-43.



- 864 37. Kelley KD, Miller KR, Todd A, Kelley AR, Tuttle R and Berberich SJ. YPEL3, a p53-  
865 regulated gene that induces cellular senescence. *Cancer Res.* 2010;70 9:3566-75.
- 866 38. Tuttle R, Simon M, Hitch DC, Maiorano JN, Hellan M, Ouellette J, et al. Senescence-  
867 associated gene YPEL3 is downregulated in human colon tumors. *Ann Surg*  
868 *Oncol.* 2011;18 6:1791-6.
- 869 39. Roth A, Adapa SR, Zhang M, Liao X, Saxena V, Goffe R, et al. Unraveling the  
870 *Plasmodium vivax* sporozoite transcriptional journey from mosquito vector to  
871 human host. *Sci Rep.* 2018;8 1:12183.
- 872 40. Zhu L, Mok S, Imwong M, Jaidee A, Russell B, Nosten F, et al. New insights into  
873 the *Plasmodium vivax* transcriptome using RNA-Seq. *Sci Rep.* 2016;6:20498.
- 874 41. Kramer S. RNA in development: how ribonucleoprotein granules regulate the life  
875 cycles of pathogenic protozoa. *WIR: RNA.* 2014;5 2:263-84.
- 876 42. Tucker RP. The thrombospondin type 1 repeat superfamily. *Int J Biochem Cell*  
877 *Biol.* 2004;36 6:969-74.
- 878 43. Ntumngia FB, Bouyou-Akotet MK, Uhlemann AC, Mordmuller B, Kremsner PG  
879 and Kun JF. Characterisation of a tryptophan-rich *Plasmodium falciparum*  
880 antigen associated with merozoites. *Mol Biochem Parasitol.* 2004;137 2:349-53.
- 881 44. Gubbels MJ, Vaishnav S, Boot N, Dubremetz JF and Striepen B. A MORN-repeat  
882 protein is a dynamic component of the *Toxoplasma gondii* cell division  
883 apparatus. *J Cell Sci.* 2006;119 Pt 11:2236-45.
- 884 45. Aly AS, Lindner SE, MacKellar DC, Peng X and Kappe SH. SAP1 is a critical post-  
885 transcriptional regulator of infectivity in malaria parasite sporozoite stages. *Mol*  
886 *Microbiol.* 2011;79 4:929-39.
- 887 46. Okano H, Imai T and Okabe M. Musashi: a translational regulator of cell fate.  
888 *Journal of Cell Science.* 2002;115 7:1355-9.
- 889 47. Cui L, Lindner S and Miao J. Translational regulation during stage transitions in  
890 malaria parasites. *Annals NY Acad Sci.* 2015;1342 1:1-9.
- 891 48. Lasko P. Gene regulation at the RNA layer: RNA binding proteins in intercellular  
892 signaling networks. *Sci STKE.* 2003;179:RE6.
- 893 49. Guizetti J and Scherf A. Silence, activate, poise and switch! Mechanisms of  
894 antigenic variation in *Plasmodium falciparum*. *Cell microbiol.* 2013;15 5:718-26.
- 895 50. Wu Q, Bruce AW, Jedrusik A, Ellis PD, Andrews RM, Langford CF, et al. CARM1 is  
896 required in embryonic stem cells to maintain pluripotency and resist  
897 differentiation. *Stem Cells.* 2009;27 11:2637-45.
- 898 51. Shi S and Ehrt S. Dihydrolipoamide acyltransferase is critical for *Mycobacterium*  
899 *tuberculosis* pathogenesis. *Infect Immun.* 2006;74 1:56-63.
- 900 52. Ma C, Sim S, Shi W, Du L, Xing D and Zhang Y. Energy production genes *sucB* and  
901 *ubiF* are involved in persister survival and tolerance to multiple antibiotics and  
902 stresses in *Escherichia coli*. *FEMS Microbiol Lett.* 2010;303 1:33-40.
- 903 53. Schrader J, Moyle R, Bhalerao R, Hertzberg M, Lundeborg J, Nilsson P, et al.  
904 Cambial meristem dormancy in trees involves extensive remodelling of the  
905 transcriptome. *Plant J.* 2004;40 2:173-87.
- 906 54. Yazawa K and Kamada H. Identification and characterization of carrot HAP  
907 factors that form a complex with the embryo-specific transcription factor C-  
908 LEC1. *J Exp Bot.* 2007;58 13:3819-28.
- 909 55. Wood FC, Heidari A and Tekle YI. Genetic Evidence for Sexuality in  
910 *Cochliopodium* (Amoebozoa). *J Hered.* 2017;108 7:769-79.
- 911 56. Voorberg-van der Wel A, Roma G, Gupta DK, Schuierer S, Nigsch F, Carbone W, et  
912 al. A comparative transcriptomic analysis of replicating and dormant liver stages  
913 of the relapsing malaria parasite *Plasmodium cynomolgi*. *Elife.* 2017;6
- 914 57. Lopez-Rubio J-J, Mancio-Silva L and Scherf A. Genome-wide analysis of  
915 heterochromatin associates clonally variant gene regulation with perinuclear  
916 repressive centers in malaria parasites. *Cell host & microbe.* 2009;5 2:179-90.

- 917 58. Duffy MF, Selvarajah SA, Josling GA and Petter M. Epigenetic regulation of the  
918 *Plasmodium falciparum* genome. Brief Funct Genomics. 2014;13 3:203-16.
- 919 59. Cui L, Miao J, Furuya T, Li X, Su XZ and Cui L. PfGCN5-mediated histone H3  
920 acetylation plays a key role in gene expression in *Plasmodium falciparum*.  
921 Eukaryot Cell. 2007;6 7:1219-27.
- 922 60. Rovira-Graells N, Gupta AP, Planet E, Crowley VM, Mok S, de Pouplana LR, et al.  
923 Transcriptional variation in the malaria parasite *Plasmodium falciparum*.  
924 Genome research. 2012;22 5:925-38.
- 925 61. De Silva EK, Gehrke AR, Olszewski K, León I, Chahal JS, Bulyk ML, et al. Specific  
926 DNA-binding by apicomplexan AP2 transcription factors. Proc Nat'l Acad Sci.  
927 2008;105 24:8393-8.
- 928 62. Painter HJ, Campbell TL and Llinás M. The Apicomplexan AP2 family: integral  
929 factors regulating *Plasmodium* development. Mol Biochem Parasitol. 2011;176  
930 1:1-7.
- 931 63. Kafsack BF, Rovira-Graells N, Clark TG, Bancells C, Crowley VM, Campino SG, et  
932 al. A transcriptional switch underlies commitment to sexual development in  
933 human malaria parasites. Nature. 2014;507 7491:248.
- 934 64. Iwanaga S, Kaneko I, Kato T and Yuda M. Identification of an AP2-family protein  
935 that is critical for malaria liver stage development. PLoS One. 2012;7 11:e47557.
- 936 65. Boden SA, Kavanova M, Finnegan EJ and Wigge PA. Thermal stress effects on  
937 grain yield in *Brachypodium distachyon* occur via H2A.Z-nucleosomes. Genome  
938 Biol. 2013;14 6:R65.
- 939 66. Kennedy M, Fishbaugher ME, Vaughan AM, Patrapuvich R, Boonhok R,  
940 Yimamnuaychok N, et al. A rapid and scalable density gradient purification  
941 method for *Plasmodium* sporozoites. Malar J. 2012;11:421.
- 942 67. Bolger AM, Lohse M and Usadel B. Trimmomatic: a flexible trimmer for Illumina  
943 sequence data. Bioinformatics (Oxford, England). 2014;30 15:2114-20.
- 944 68. Langmead B and Salzberg SL. Fast gapped-read alignment with Bowtie 2. Nat  
945 Methods. 2012;9 4:357-9.
- 946 69. Li B and Dewey CN. RSEM: accurate transcript quantification from RNA-Seq data  
947 with or without a reference genome. BMC bioinformatics. 2011;12 1:323.
- 948 70. Okonechnikov K, Conesa A and Garcia-Alcalde F. Qualimap 2: advanced multi-  
949 sample quality control for high-throughput sequencing data. Bioinformatics  
950 (Oxford, England). 2016;32 2:292-4.
- 951 71. Nikolayeva O and Robinson MD. edgeR for differential RNA-seq and ChIP-seq  
952 analysis: an application to stem cell biology. Methods Mol Biol. 2014;1150:45-  
953 79.
- 954 72. Ritchie ME, Phipson B, Wu D, Hu Y, Law CW, Shi W, et al. limma powers  
955 differential expression analyses for RNA-sequencing and microarray studies.  
956 Nucleic Acids Res. 2015;43 7:e47-e.
- 957 73. Wickham H. ggplot: An implementation of the Grammar of Graphics in R, 2006. R  
958 package version 04 0.
- 959 74. Wickham H and Chang W. ggplot2: An implementation of the Grammar of  
960 Graphics. R package version 07, URL: [http://CRAN](http://CRAN.R-project.org/package=ggplot2)  
961 [R-project org/package=](http://CRAN.R-project.org/package=ggplot2)  
962 [ggplot2](http://CRAN.R-project.org/package=ggplot2). 2008.
- 962 75. Warnes GR, Bolker B, Bonebakker L, Gentleman R, Huber W, Liaw A, et al. gplots:  
963 Various R programming tools for plotting data. R package version. 2009;2 4:1.
- 964 76. Law CW, Alhamdoosh M, Su S, Smyth GK and Ritchie ME. RNA-seq analysis is  
965 easy as 1-2-3 with limma, Glimma and edgeR. F1000Research. 2016;5.
- 966 77. Martin M. Cutadapt removes adapter sequences from high-throughput  
967 sequencing reads. EMBnet journal. 2011;17 1:pp. 10-2.
- 968 78. Li H, Handsaker B, Wysoker A, Fennell T, Ruan J, Homer N, et al. The Sequence  
969 Alignment/Map format and SAMtools. Bioinformatics (Oxford, England).  
970 2009;25 16:2078-9.

- 971 79. Zhang Y, Liu T, Meyer CA, Eeckhoutte J, Johnson DS, Bernstein BE, et al. Model-  
972 based analysis of ChIP-Seq (MACS). *Genome Biol.* 2008;9 9:R137.  
973 80. Quinlan AR and Hall IM. BEDTools: a flexible suite of utilities for comparing  
974 genomic features. *Bioinformatics (Oxford, England)*. 2010;26 6:841-2.  
975 81. Bailey TL. DREME: motif discovery in transcription factor ChIP-seq data.  
976 *Bioinformatics (Oxford, England)*. 2011;27 12:1653-9.  
977 82. Trapnell C, Roberts A, Goff L, Pertea G, Kim D, Kelley DR, et al. Differential gene  
978 and transcript expression analysis of RNA-seq experiments with TopHat and  
979 Cufflinks. *Nat Protoc.* 2012;7 3:562-78.

980 **Figure Legends:**

981 **Fig. 1** Transcriptional activity of the *P. vivax* sporozoite and evidence for translational  
982 repression. **a** Relative transcript abundance of key marker genes for sporozoites inferred by  
983 RNA-seq and qPCR (here) relative to previously published microarray data [24]; **b** Relative  
984 proportion of genes detectable as transcripts and proteins or transcripts only in RNA-seq and  
985 previously published proteomic data. Dashed line shows cut-off used in the current study for  
986 putatively repressed transcripts. Immunofluorescent staining of select proteins either known  
987 (UIS4) or predicted here (LISP1, EXP1 and ACP) to be translationally repressed in  
988 sporozoites in **c** sporozoite stages. CSP, mTIP as known positive controls and TRAP and BIP  
989 as experimental positive controls and **d** liver stages (schizonts) at 7 days post-infection in  
990 HuHep mice. Liver expression of EXP1 and ACP has been demonstrated by IFA in  
991 Mikolajczak et al [13], using the same antibodies as used here.

992  
993 **Fig. 2** Differential transcription between *Plasmodium vivax* salivary-gland sporozoites and  
994 blood-stages. **A** BCV plot showing separation between blood-stage (black) and salivary-gland  
995 sporozoite (red) biological replicates. **B** Volcano plot of distribution of fold-changes (FC) in  
996 transcription between blood-stages and salivary-gland sporozoites relative to statistical  
997 significance threshold (False Discovery Rate (FDR)  $\leq$  0.05). Positive FC represents up-  
998 regulated transcription in the sporozoite stage. **C** Mirror plot showing pFam domains  
999 statistically significantly (FDR  $\leq$  0.05) over-represented in salivary-gland sporozoite up-  
1000 regulated (red) or blood-stage up-regulated (black) transcripts. Scale bar truncated for  
1001 presentation. \* - 55 PRESAN domains are in this dataset. \*\* - 99 Vir domains are in this  
1002 dataset.

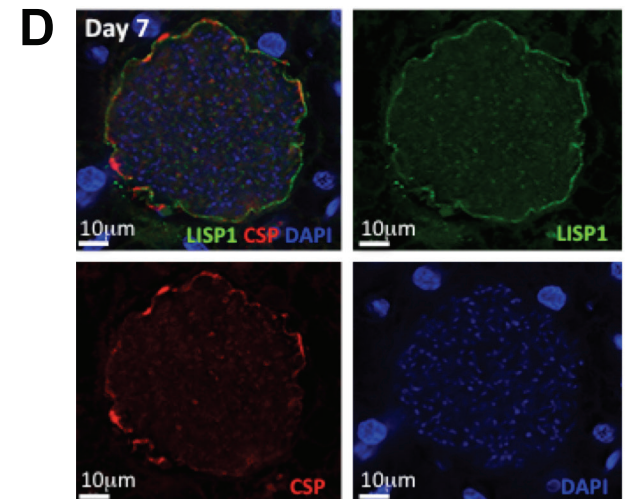
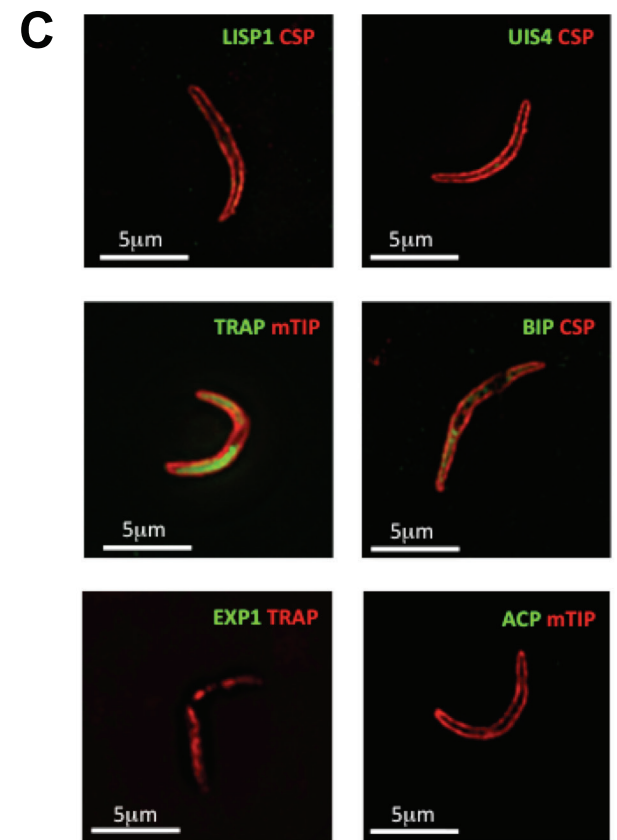
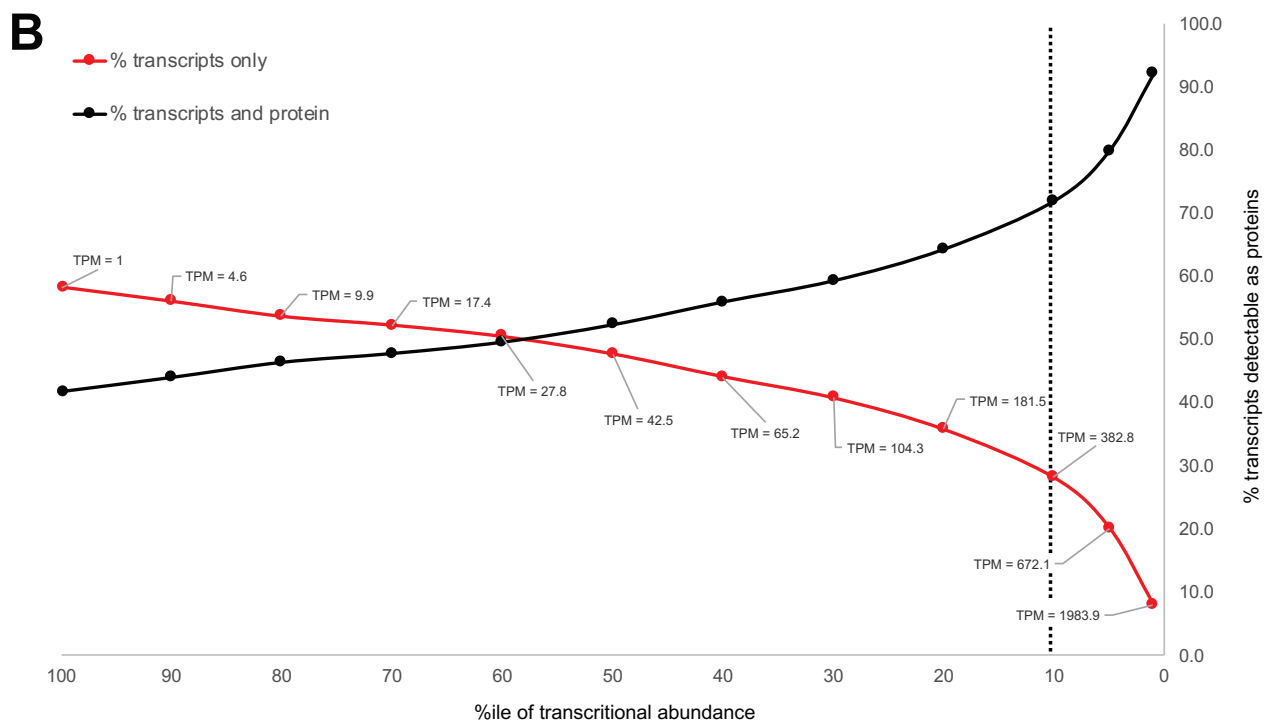
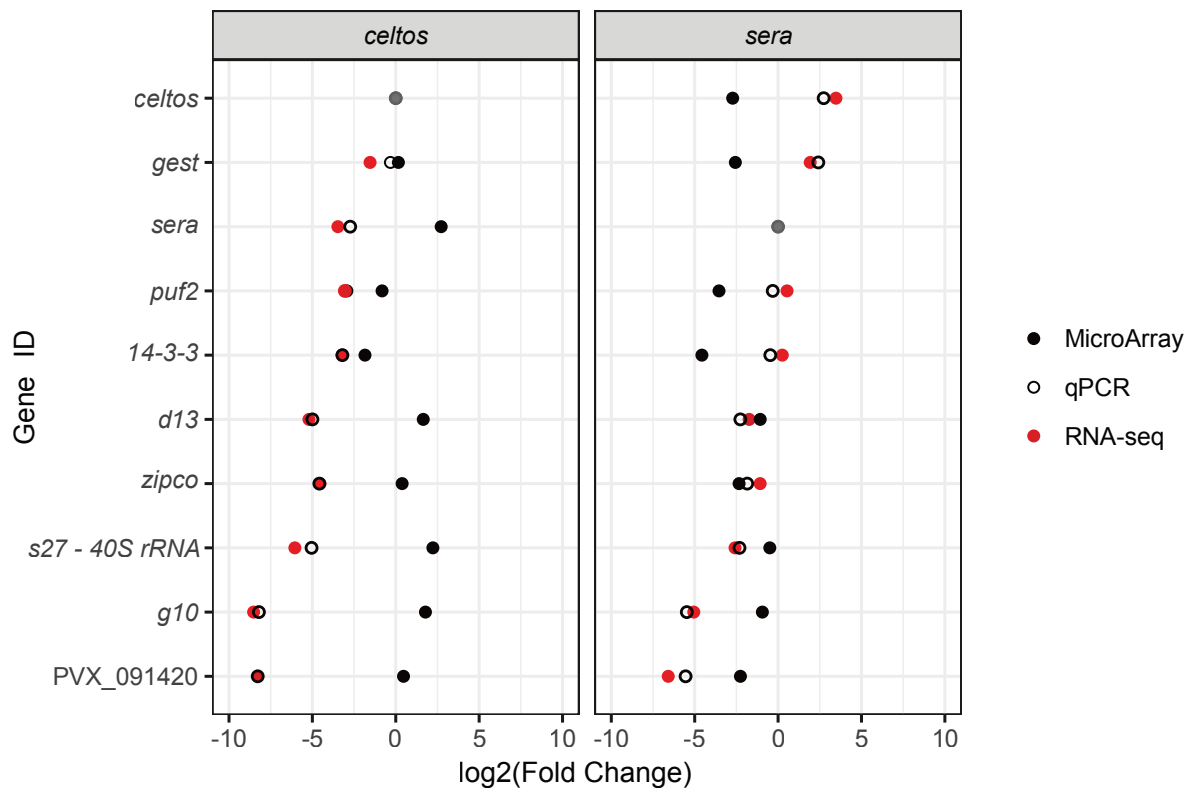
1003  
1004 **Fig. 3** Differential transcription between *P. vivax* sporozoites (SPZ), mixed (mLS) and  
1005 hypnozoite (HPZ) enriched liver stages (liver-stage data from Gural et al [22]). **A** Heatmap  
1006 comparisons showing summed transcription of enriched Pfa domains in HPZ vs mLS (left),  
1007 SPZ vs HPZ (top middle) and SPZ vs mLS (top right) comparisons. All Pfa domains  
1008 statistically significantly enriched at p-value 0.05). All transcript data for stage up-regulated  
1009 genes at FDR 0.01). **B** Violin box-plot showing relative fold-change differences between SPZ  
1010 and HPZ compared with SPZ and mLS for genes down-regulated in mLS compared to SPZ,  
1011 but not down-regulated in HPZ compared to SPZ. **C** Ternary heatmap summarizing relative  
1012 transcript abundance in each of SPZ, mLS and HPZ stages.

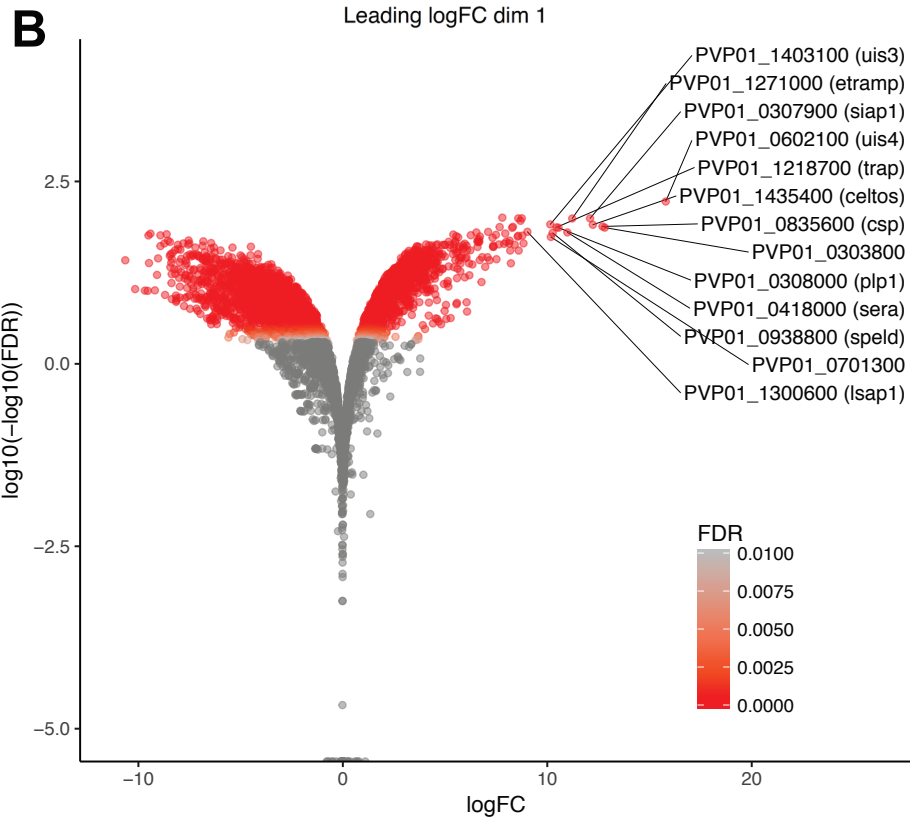
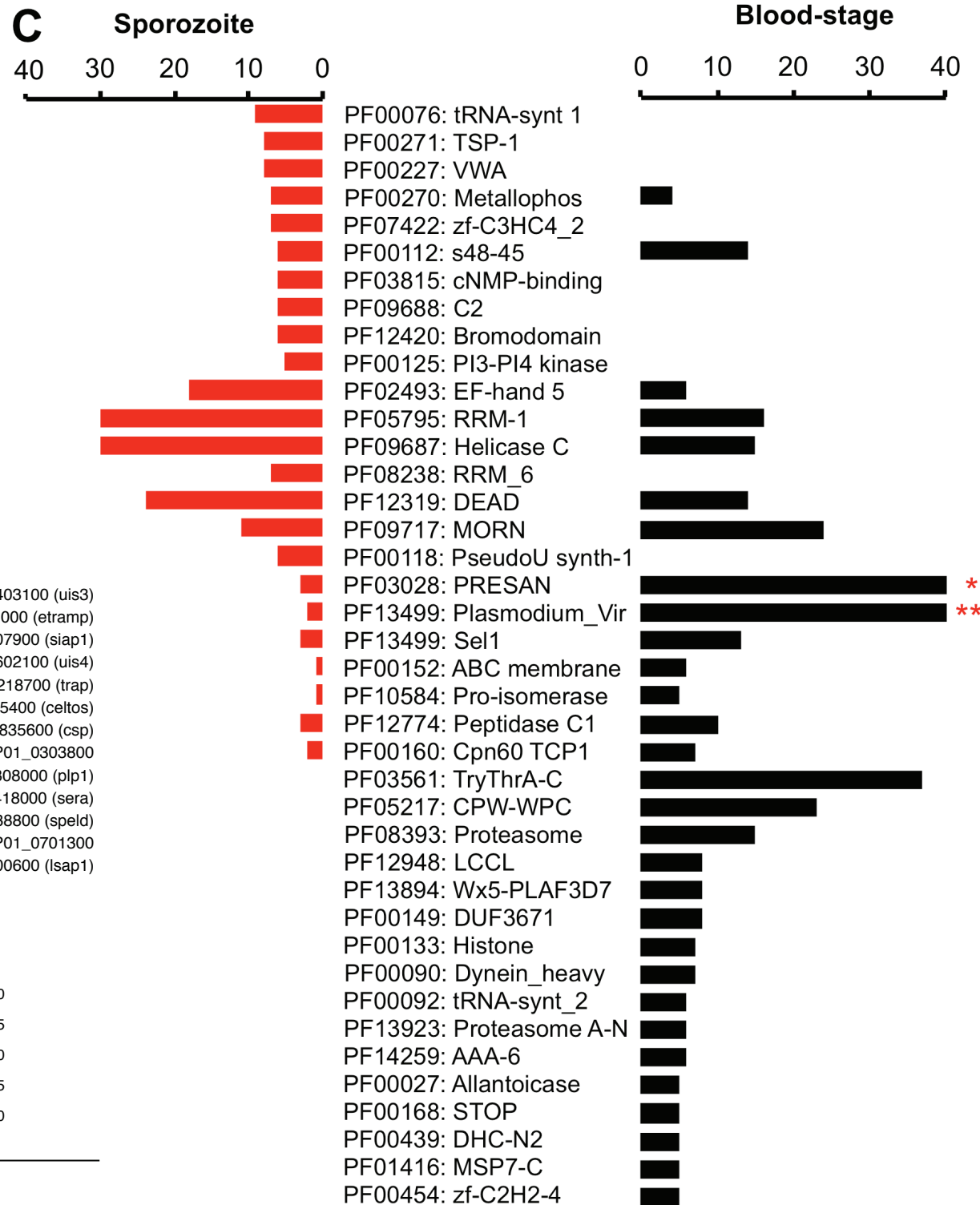
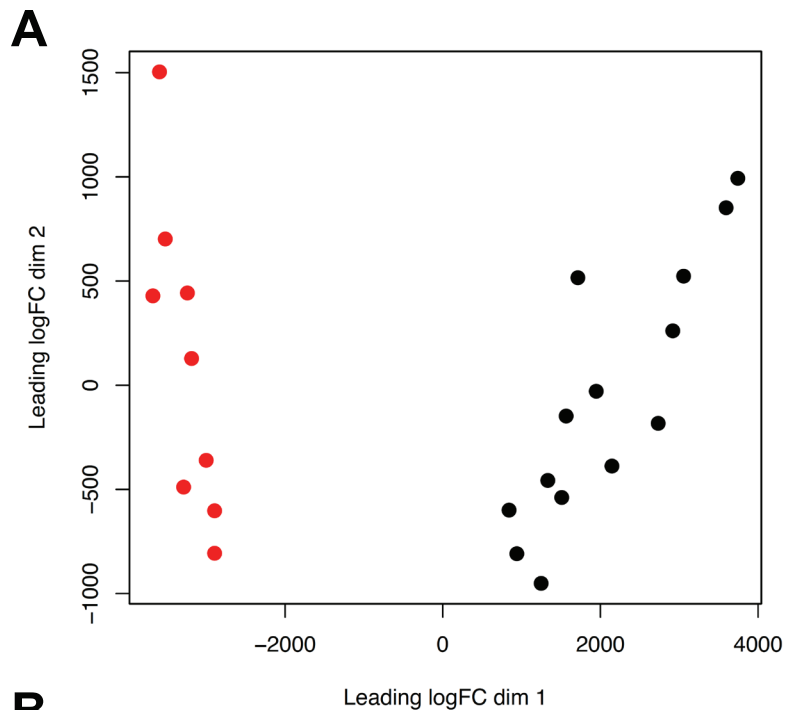
1013  
1014 **Fig. 4** Histone epigenetics relative to transcriptional behaviour in salivary-gland sporozoites.  
1015 **a** Representative H3K9me3, H3K4me3 and H3K9ac ChIP-seq data (grey) from a  
1016 representative chromosome (*P. vivax* P01 Chr5) relative to mRNA transcription in salivary-  
1017 gland sporozoites (black) and blood-stages (black). Small numbers to top left of each row  
1018 show data range. **b** Salivary-gland sporozoite transcription relative to nearest stable histone  
1019 epigenetic marks. Numbers at the top of the figure represent total genes included in each  
1020 category. Numbers within in box plot represent mean transcription in transcripts per million  
1021 (TPM). **c** Sequence motifs enriched within 1kb upstream of the Transcription Start Site of  
1022 highly transcribed (top 10%) relative to lowly transcribed genes associated with H3K9ac  
1023 marks in salivary-gland sporozoites. **d** Relative transcription of (sub)telomeric genes in *P.*  
1024 *vivax* salivary-gland sporozoites and blood-stages categorized by gene sets up-regulated in

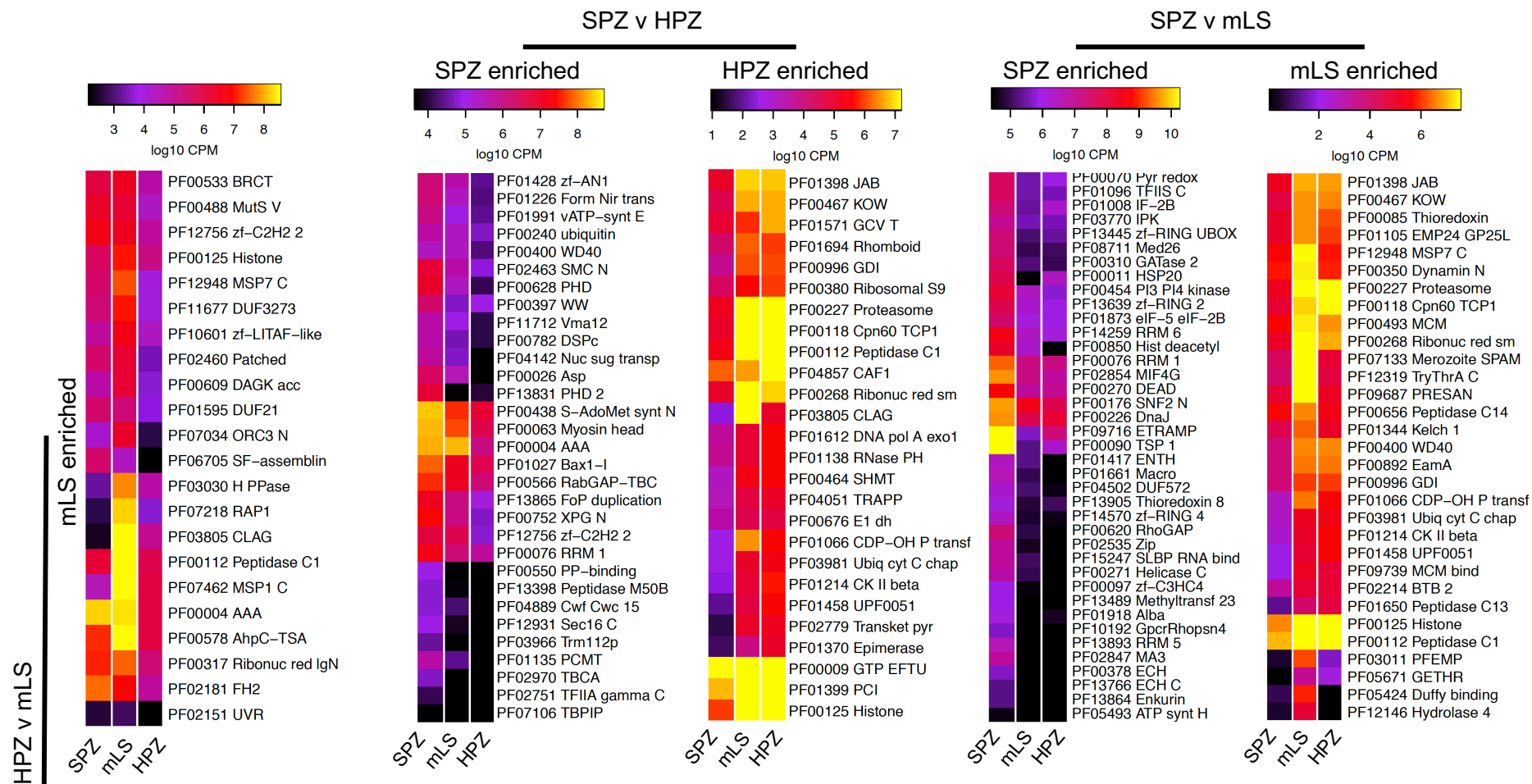
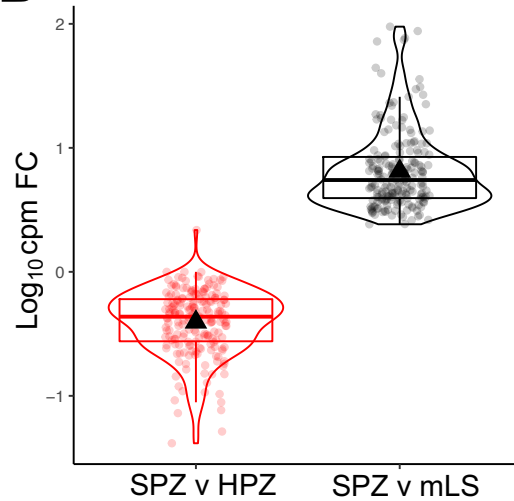
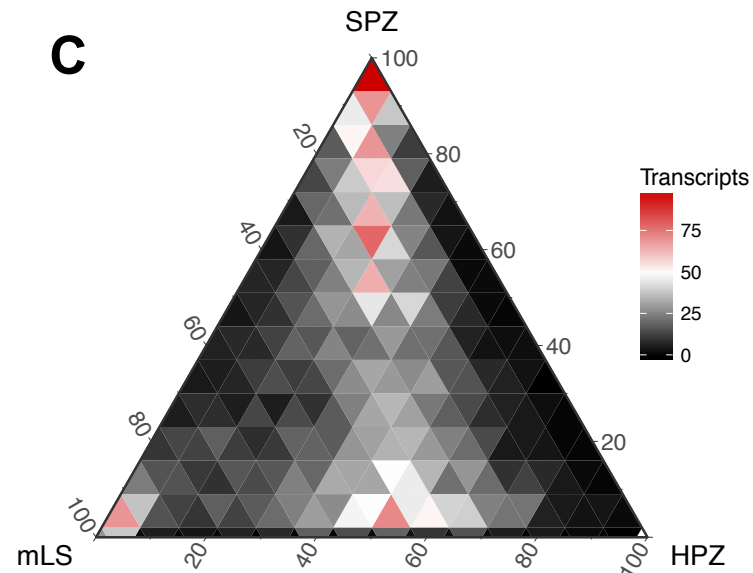
1025 blood-stages (blue), salivary sporozoites (red) or not stage enriched (grey). Numbers in each  
1026 box show mean transcription in TPM.

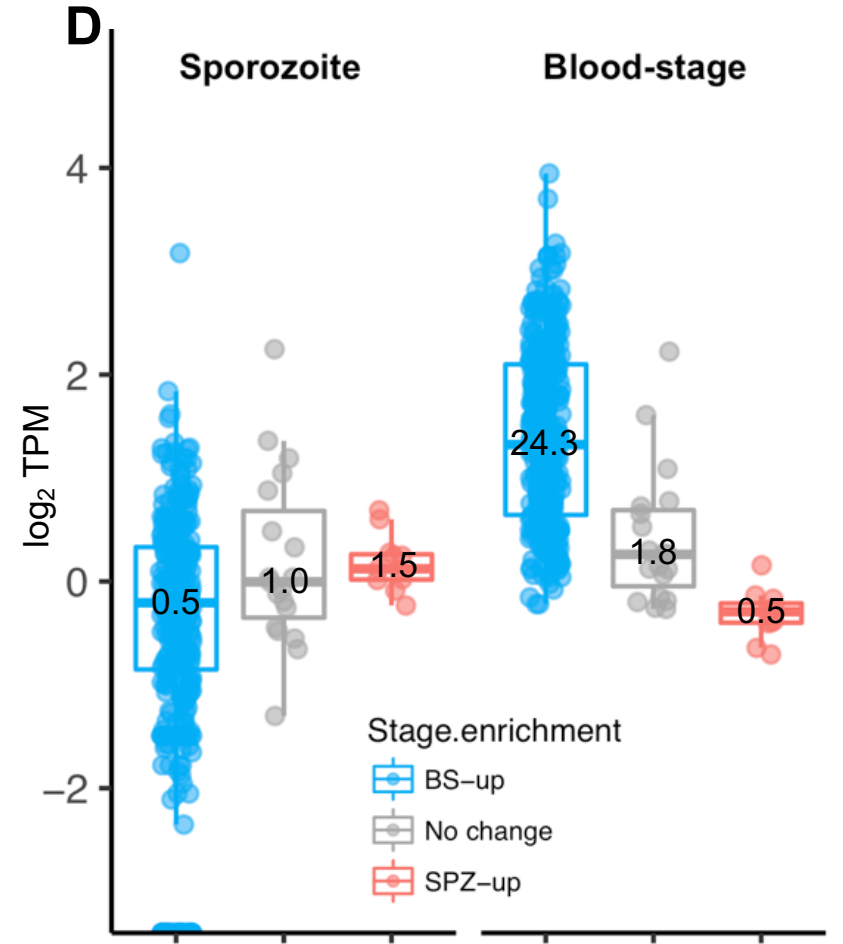
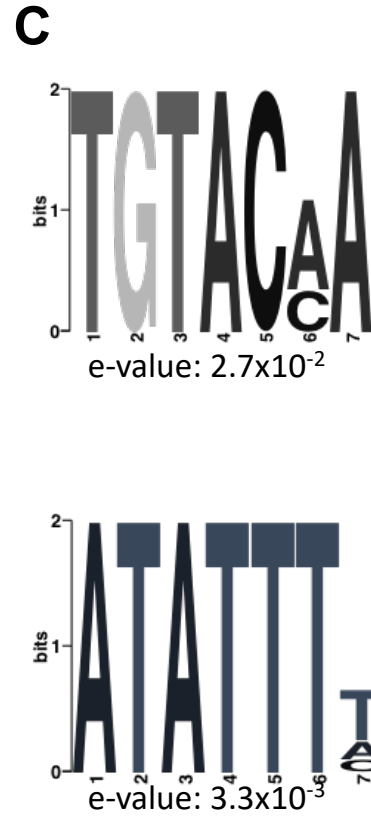
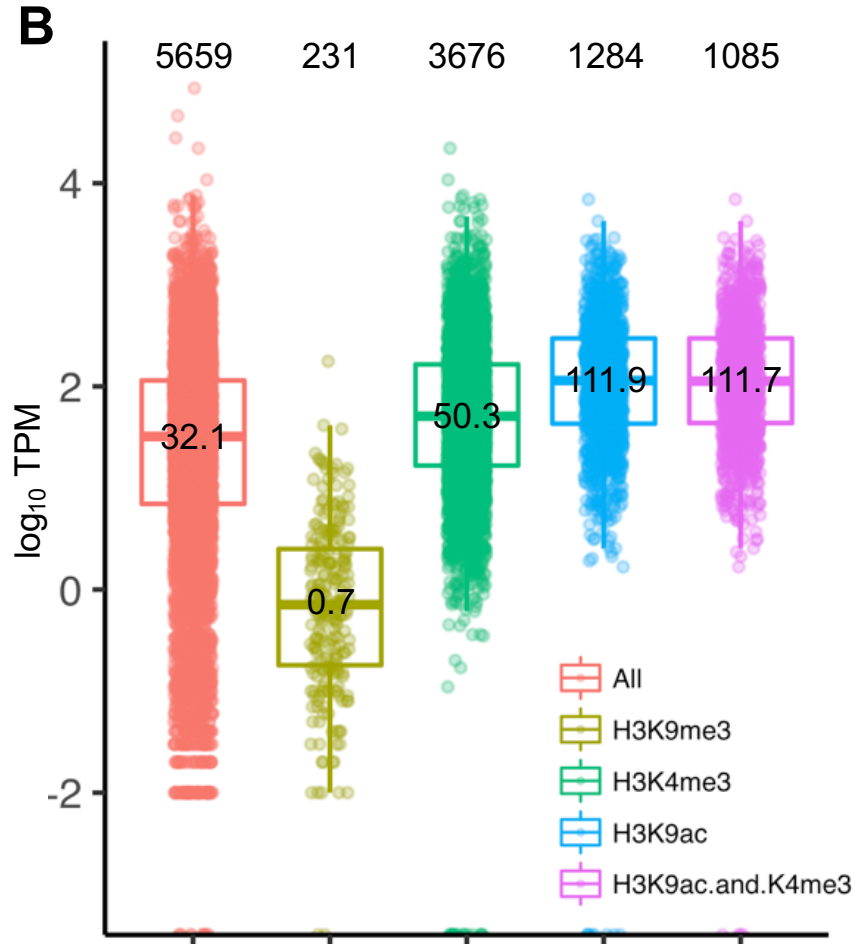
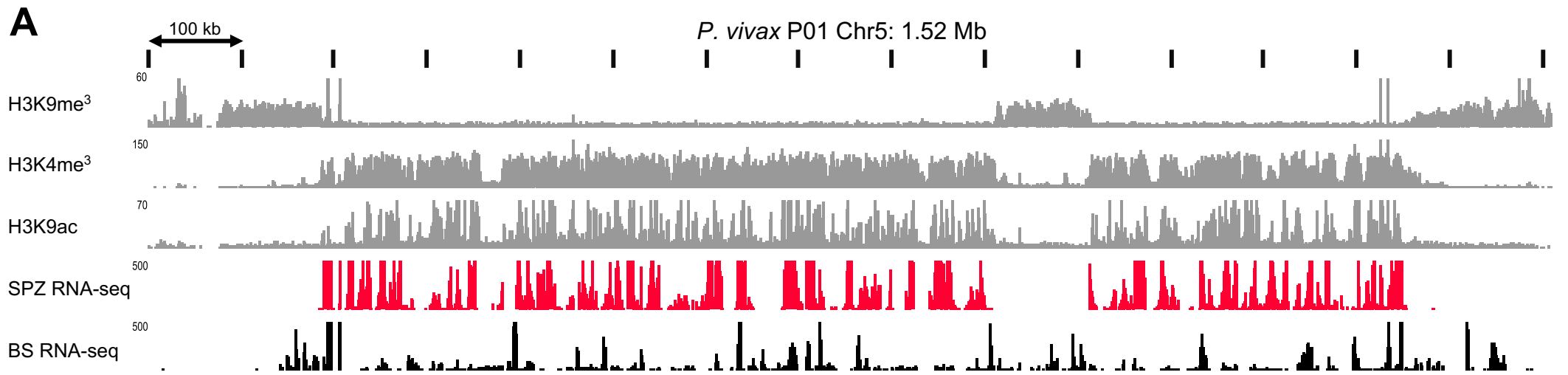
1027

1028 **Fig. 5** Schematic of potential mechanisms underpinning development in differentiation of *P.*  
1029 *vivax* sporozoites during liver-stage infection as hypnozoites and schizonts. We suggest  
1030 differentiation programming at different points in development; first, schizont or hypnozoite  
1031 fate possibly encoded in the sporozoite as epigenetic signals or translationally repressed  
1032 transcripts; secondly, suppression signals that halt progression of the hypnozoite to schizont  
1033 stage and support persistence; and finally activation signals signified by a release in  
1034 chromatin, (post)transcriptional and (post)translational control leading to up-regulation of  
1035 replication, metabolic and protein export pathways.





**A****B****C**





## DIFFERENTIATION

- **Translational repressors**  
e.g., Puf2, Alba2/4, HOMU, Yippee, Zipco
- **Invasion**  
e.g., Celtos, Gest
- **Liver development**  
e.g., LISP1, LISP2, ETRAMPS, TRAP
- **Transcription factors**  
e.g., AP2-SP2, AP2-L, AP2-Q?

## SUPPRESSION

- **Metabolic/replication suppressors**  
e.g., sucB, HAP2, MAK16
- **Histone arginine methylation**  
e.g., CARM1, EEML2
- **Protein translation**  
e.g., eIF-3H, Puf1

## ACTIVATION

- **Merozoite development**  
e.g., MSP1, MSP3, MSP9
- **Rhoptry function**  
e.g., RAP1, RNP2, RNP3
- **Reticuocyte binding**  
e.g., RBP2a, RBP2b, RBP2C
- **Exported Proteins**  
e.g., PHISTs

